



Deposited via The University of Sheffield.

White Rose Research Online URL for this paper:

<https://eprints.whiterose.ac.uk/id/eprint/100955/>

Version: Accepted Version

Article:

Gokul, J.K., Hodson, A.J., Saetnan, E.R. et al. (2016) Taxon interactions control the distributions of cryoconite bacteria colonizing a High Arctic ice cap. *Molecular Ecology*, 25 (15). pp. 3752-3767. ISSN: 0962-1083

<https://doi.org/10.1111/mec.13715>

This is the peer reviewed version of the following article: Gokul, J.K., Hodson, A.J., Saetnan, E.R., Irvine-Fynn, T.D., Westall, P.J., Detheridge, A.P., Takeuchi, N., Bussell, J., Mur, L.A. and Edwards, A. (2016) Taxon interactions control the distributions of cryoconite bacteria colonizing a High Arctic ice cap. *Molecular Ecology*, which has been published in final form at <http://dx.doi.org/10.1111/mec.13715>. This article may be used for non-commercial purposes in accordance with Wiley Terms and Conditions for Self-Archiving (<http://olabout.wiley.com/WileyCDA/Section/id-828039.html>)

Reuse

Items deposited in White Rose Research Online are protected by copyright, with all rights reserved unless indicated otherwise. They may be downloaded and/or printed for private study, or other acts as permitted by national copyright laws. The publisher or other rights holders may allow further reproduction and re-use of the full text version. This is indicated by the licence information on the White Rose Research Online record for the item.

Takedown

If you consider content in White Rose Research Online to be in breach of UK law, please notify us by emailing eprints@whiterose.ac.uk including the URL of the record and the reason for the withdrawal request.

**Taxon interactions control the distributions of cryoconite
bacteria colonizing a High Arctic ice cap**

Journal:	<i>Molecular Ecology</i>
Manuscript ID	MEC-15-1529.R1
Manuscript Type:	Original Article
Date Submitted by the Author:	n/a
Complete List of Authors:	Gokul, Jarishma; Aberystwyth University, Institute of Biological, Environmental & Rural Sciences Hodson, Andrew; University of Sheffield, Geography; Universitetscenteret pa Svalbard AS, Arctic Geology Saetnan, Eli; Aberystwyth University, Institute of Biological, Environmental & Rural Sciences Irvine-Fynn, Tristram; Aberystwyth University, Geography and Earth Sciences Westall, Phillipa; Aberystwyth University, Institute of Biological, Environmental and Rural Sciences Detheridge, Andrew; Aberystwyth University, Institute of Biological, Environmental and Rural Sciences Takeuchi, Nozomu; Chiba University, Department of Earth Sciences Bussell, Jennifer; University of Nottingham Mur, Luis; Aberystwyth University, Institute of Biological, Environmental and Rural Sciences Edwards, Arwyn; Aberystwyth University, IBERS
Keywords:	Svalbard, cryoconite, biogeography, ecosystem engineering, keystone species, Bacteria

1 Taxon interactions control the distributions of cryoconite bacteria colonizing a
2 High Arctic ice cap

3 Jarishma K. Gokul¹, Andrew J. Hodson^{2,3}, Eli R. Saetnan¹, Tristram D.L., Irvine-Fynn⁴,
4 Philippa J. Westall¹, Andrew P. Detheridge¹, Nozomu Takeuchi⁵, Jennifer Bussell^{1,6} Luis A.J.
5 Mur¹, Arwyn Edwards*¹.

6
7 Postal Address: ¹Institute of Biological, Rural and Environmental Sciences, Cledwyn
8 Building, Aberystwyth University, Aberystwyth, UK. ²Department of Geography, University
9 of Sheffield, Sheffield, UK. ³Department of Arctic Geology, University Centre in Svalbard
10 (UNIS), Longyearbyen, Svalbard. ⁴Department of Geography and Earth Sciences,
11 Aberystwyth University, Llandinam Building, Aberystwyth, UK. ⁵Department of Earth
12 Sciences, Graduate School of Science, Chiba University, 1-33, Yayoicho, Inage-ku, Chiba,
13 Japan. ⁶University of Nottingham, Sutton Bonington Campus, Loughborough, Leicestershire,
14 LE12 5RD.

15

16 Keywords: Svalbard / Cryoconite / biogeography / ecosystem engineering / keystone species /
17 bacteria

18 *Corresponding Author: Arwyn Edwards, Institute of Biological, Rural and Environmental
19 Sciences, Aberystwyth University, Aberystwyth, UK aye@aber.ac.uk

20

21 Running title: Bacterial biogeography of a High Arctic ice cap.

22 Abstract (247 words)

23 Microbial colonization of glacial ice surfaces incurs feedbacks which affect the melting rate
24 of the ice surface. Ecosystems formed as microbe-mineral aggregates termed cryoconite
25 locally reduce ice surface albedo and represent foci of biodiversity and biogeochemical
26 cycling. Consequently, greater understanding the ecological processes in the formation of
27 functional cryoconite ecosystems upon glacier surfaces is sought. Here we present the first
28 bacterial biogeography of an ice cap, evaluating the respective roles of dispersal,
29 environmental and biotic filtration occurring at local scales in the assembly of cryoconite
30 microbiota. 16S rRNA gene amplicon semiconductor sequencing of cryoconite colonizing a
31 Svalbard ice cap coupled with digital elevation modelling of physical parameters reveals the
32 bacterial community is dominated by a ubiquitous core of generalist taxa, with evidence for a
33 moderate pairwise distance-decay relationship. While geographic position and melt season
34 duration are prominent among environmental predictors of community structure, the core
35 population of taxa appears highly influential in structuring the bacterial community. Taxon
36 co-occurrence network analysis reveals a highly modular community structured by positive
37 interactions with bottleneck taxa, predominantly *Actinobacteria* affiliated to isolates from soil
38 humus. In contrast, the filamentous cyanobacterial taxon (assigned to *Leptolyngbya*) which
39 dominates the community and bind together granular cryoconite are poorly connected to other
40 taxa. While our study targeted one ice cap, the prominent role of generalist core taxa with
41 close environmental relatives across the global cryosphere indicate discrete roles for
42 cosmopolitan *Actinobacteria* and *Cyanobacteria* as respective keystone taxa and ecosystem
43 engineers of cryoconite ecosystems colonizing ice caps.

44

45

46 INTRODUCTION

47 The interactions of glacial systems with climate, water and landscape assume considerable
48 scientific and societal concern. This interest pre-dates the appreciation that glaciers, ice caps
49 and ice sheets comprise microbial ecosystems (Hodson *et al.* 2008). Indeed, the activities of
50 biodiverse microbial ecosystems associated with glacial habitats interact with both the
51 dynamics of glacial systems and influence biogeochemical cycles (Edwards *et al.* 2014a;
52 Hood *et al.* 2015; Rime *et al.* 2015). At the glacier surface, cryoconite ecosystems are
53 recognized as major foci of microbial biodiversity and activity (Cameron *et al.* 2012; Cook *et*
54 *al.* 2015b; Edwards *et al.* 2011) which influence ice surface albedo (Bøggild 1997; Takeuchi
55 2002) and potentially ice topography (Cook *et al.* 2015a).

56 The darkening action of granular microbe-mineral aggregates, termed cryoconite, upon ice
57 surfaces causes localized melting and so cryoconite ecosystems often occupy quasi-circular
58 holes within the ice surface which interact with the hydrology of the porous ice surface (Cook
59 *et al.* 2015c; Edwards *et al.* 2011). The cryoconite biota includes viruses, bacteria, fungi,
60 other micro-eukaryotes and meiofauna (Sävström *et al.* 2002) which actively contribute to
61 carbon and nitrogen cycling (Hodson *et al.* 2007; Segawa *et al.* 2014). On both Arctic and
62 alpine glaciers, the composition and structure of cryoconite bacterial communities are closely
63 related to the rates of microbial activities and the composition of cryoconite organic matter
64 (Edwards *et al.* 2011; Edwards *et al.* 2014b; Edwards *et al.* 2013a). It appears that
65 filamentous cyanobacteria (e.g. *Phormidium*, *Phormidesmis* or *Leptolyngbya* sp.) aggregate
66 aeolian debris (Hodson *et al.* 2010; Langford *et al.* 2010), engineering the formation of
67 granular cryoconite forming microbial communities distinctive from proximal habitats
68 (Edwards *et al.* 2013b; Musilova *et al.* 2015). While the role of filamentous cyanobacteria is
69 pivotal to the formation of stable cryoconite granules (Langford *et al.* 2010) harbouring a

70 diverse community of bacterial heterotrophs, whether cyanobacteria represent keystone
71 species or ecosystem engineers is equivocal (Edwards *et al.* 2014b). Similarly, while
72 commonly-occurring taxa in a given habitat, termed the core taxa, are assumed to regulate
73 ecosystem functioning, and rare taxa (present within the long tail of a taxon abundance curve)
74 may represent a store of genomic and functional variability as a “seed bank” (Fuhrman 2009,
75 whether core and tail taxa in cryoconite bacterial communities occur as generalists and
76 specialists with broad- and narrow- shaped niches respectively {Barberan, 2012 #833; Pedrós-
77 Alió 2006) is poorly defined. Understanding the topology of the network of interactions
78 between taxa varying in abundance and ubiquity (Barberan *et al.* 2012; Peura *et al.* 2015;
79 Steele *et al.* 2011) can therefore be expected to enhance our understanding of how cryoconite
80 bacterial communities colonize ice surfaces, accumulating organic matter and accelerating ice
81 melt (Cook *et al.* 2015a; Cook *et al.* 2015b).

82 Moreover, while previous studies have shown clear evidence of inter-regional and inter-
83 glacier differences in cryoconite bacterial communities (Cameron *et al.* 2012; Edwards *et al.*
84 2011) the drivers and extent of spatial variation within the scale of individual glaciers are
85 unclear. Recently, Langford *et al.* (2014) conducted a high-resolution sampling of cryoconite
86 properties on a single Svalbard valley glacier, finding only moderate evidence for changes in
87 the properties of cryoconite granules across the ice surface. Likewise Edwards *et al.* (2011)
88 reported that inter-glacier differences outweighed very weak distance-decay relationships in
89 bacterial community structure on three Svalbard valley glaciers. Furthermore, the temporal
90 dynamics of cryoconite bacterial communities are less clear, with contrasting inferences made
91 from intra-seasonal sampling of cryoconite ecosystems at the margin of Greenland’s ice sheet
92 in two recent studies (Musilova *et al.* 2015; Stibal *et al.* 2015).

93 Consequently, the influence of seasonal melting upon community history or the response of
94 cryoconite bacterial communities to environmental drivers prevailing within stable, low-
95 gradient ice masses is unknown. This is likely to be the consequence of truncated
96 environmental gradients associated with a low-complexity landscape responding to melt-
97 associated drivers over a short dynamic range as the melting season proceeds rapidly. While
98 studies of species turnover across elongated environmental gradients, for example at the ice
99 sheet scale, could provide further insights, these will be across a broader, potentially
100 continental, biogeographical scale since ice sheets span latitudinal and climatological
101 gradients.

102 In contrast, ice caps provide an attractive model system for exploring the biogeography of
103 microbial community development. Ice caps are defined as terrestrial ice masses which are
104 not constrained by the topography of their underlying terrain but rather are shaped principally
105 by their surface mass balance, and as distinct from ice sheets, have a surface area of less than
106 50,000 km² (Benn & Evans 2014). Consequently, by virtue of their surface topography, ice-
107 cap associated microbial communities are likely to be situated within strong local
108 environmental gradients within the same locality. Therefore, we hypothesize that the relative
109 influence of dispersal, environmental and biotic filters in the assembly of cryoconite bacterial
110 communities can be evaluated by respectively examining distance-decay relationships,
111 linkages with physical parameters and taxon interactions of ice cap cryoconite microbiota.

112 In this study, we collected cryoconite from across an entire ice cap in the High Arctic
113 archipelago of Svalbard which was constrained by a high resolution digital elevation model,
114 permitting a detailed analysis of the bacterial biogeography in relation to the topography of
115 the ice cap. We show that geographic position and melt season duration do influence
116 community structure, with evidence of a moderate distance-decay relationship in community

117 similarity and the dominance of a core population comprising generalist taxa. Co-occurrence
118 network analysis based identification of keystone species among heterotrophic bacteria rather
119 than filamentous cyanobacteria which are considered ecosystem engineers. We conclude that
120 biotic filtering (i.e. taxon-taxon interactions such as competition or cooperation) plays a
121 critical but hitherto unrecognized role in the microbial colonization of ice surfaces.

For Review Only

122 MATERIALS AND METHODS

123 Site description and Sampling

124 Foxfonna is an ice cap measuring approximately 4 km² in central Svalbard (78° 08'N, 16° 07'
125 E; Figure 1) with ice elevations ranging from ~675 to 955 m a.s.l (Rutter *et al.* 2011). The
126 ice cap dome is almost decoupled from two small outlet glaciers descending to 285 m a.s.l.:
127 Rieperbreen to the west and an unnamed outlet glacier to the north. Typically, the ice cap
128 dome experiences melt for a short (~45 day) period of the summer. Surface mass balance
129 measurements at seven stakes drilled into the ice cap indicate an average net annual balance
130 of -0.25 +/- 0.36 (s.d.) m water equivalent for the period 2007 – 2014 (Rutter *et al.*, (2011));
131 The strong variability is caused by occasional positive balance years for the ice cap, which
132 last occurred during 2008 and 2012. Cryoconite samples were collected from the dome-
133 shaped higher elevations (>700 m a.s.l.) of the ice cap on the 23rd of August 2011, towards
134 the end of an ablation season during what was a close to average net mass balance year at the
135 site (i.e. -0.38 m water equivalent). As is common at elevations proximate to the late summer
136 snow line in Svalbard (Wadham *et al.* 2006) the superimposed ice layer was decaying and
137 facilitated the development and exposure of cryoconite debris. Sampling was undertaken at
138 four sectors according to aspect (hereafter G1, G2, G3, G4) over the ice cap surface. At 37
139 locations across the ice cap, cryoconite debris was aspirated into sterile 15 mL tubes and
140 transferred on ice to -80°C frozen storage within four hours for three weeks and thereafter
141 transferred frozen in insulated containers within ten hours, to -80°C storage in the UK. The
142 surface area cover of cryoconite, termed, Apparent Cryoconite Area (ACA) was calculated as
143 previously detailed (Irvine-Fynn *et al.* 2010) while chlorophyll a was quantified from
144 cryoconite slurries as described (Langford *et al.* 2014).

145 Digital Elevation Model

146 Elevation data coupled with high-resolution aerial imagery was used to compile a digital
147 elevation model (DEM) of the ice cap surface with a 5 m horizontal resolution. Due to the
148 likely presence of noise in the raw elevation data, a standard smoothing filter was applied to
149 the DEM (Wise 2000).

150 Primary (e.g. slope, aspect) and secondary (e.g. curvature, hydrological flow) indices were
151 extracted from the smoothed DEM using ESRI's ArcGIS software. The indices describing the
152 ice cap surface character and topographic attributes were retrieved using the ArcGIS "Spatial
153 Analyst" tool-set following established recommendations (e.g. (Moore *et al.* 1991). While
154 both slope and aspect dictate solar radiation receipt at the ice surface, slope also serves as a
155 proxy for local meltwater flow velocity and an index for potential hydrological disturbance.
156 Rather than using slope as a proxy for meltwater discharge, the Flow Accumulation Area
157 (hereafter, FAA) defined as the upslope area in m² draining to location point was used to
158 represent a meltwater discharge regime. With knowledge that meltwater flow on Arctic
159 glacier surfaces occurs dominantly through a near-surface perched aquifer (Irvine-Fynn &
160 Edwards 2013; Irvine-Fynn *et al.* 2011), the topographic wetness index as a function of FAA
161 and slope provides a continuous descriptor for areas over the ice cap likely considered to
162 range between well-drained or water-saturated. The convex nature of the ice cap surface
163 rendered use of the d8 algorithm (Jenson & Domingue) more appropriate than alternatives
164 (e.g. Tarboton (1997)) for prescribing flow routing over the ice cap surface.

165

166 Additional indices describing the surface conditions were calculated from the DEM. Potential
167 incident radiation (IR) receipt for all locations across the ice cap throughout the summer melt

168 season in 2011 was calculated following standard algorithms (Irvine-Fynn *et al.* 2014). Local
169 variability in cloud cover precluded accurate, distributed estimations of actual radiation
170 receipt at each sample site. However, spatially distributed air temperature records were
171 extrapolated from data collected at the weather station on the outlet glacier to the north of
172 Foxfonna (Figure 1) using a local air temperature lapse rate of $-0.65\text{ }^{\circ}\text{C}$ per 100 m elevation.
173 Measures of melt intensity in the form of a count of hours $> 0^{\circ}\text{C}$ (PositiveHrs), positive
174 degree days (PDDs) and positive degree hours (PDHrs; see (Hock 2005)) were derived from
175 the extrapolated weather station record.

176 This range of environmental parameters were extracted from the DEM for each sample site
177 and normalized in Primer6/PERMANOVA+ (PRIMER-E Ltd) for use with multivariate
178 analyses.

179 Sample handling and DNA Extraction

180 All samples were handled in a bleach-decontaminated laminar flow hood using sterile tools
181 and certified DNA free plasticware as previously detailed (Edwards *et al.* 2011). Negative
182 extraction and PCR controls were included to verify the absence of contamination based upon
183 the absence of a band upon gel electrophoresis, but not sequenced. Community genomic DNA
184 was extracted from 0.5g of wet cryoconite using a CTAB/Phenol - chloroform bead-beating
185 based extraction and polyethylene glycol precipitation (Griffiths *et al.* 2000) as previously
186 described (Hill *et al.* 2015) and detailed in **supplementary methods**. Reagents were DEPC-
187 treated and autoclaved. DNA quality checks by agarose gel and preliminary 16S rRNA gene
188 T-RFLP were performed as described previously (Edwards *et al.* 2014b) and extraction and
189 negative template controls did not yield product.

190 16S ribosomal RNA gene amplicon semiconductor sequencing

191 Bacterial 16S rRNA gene regions were PCR amplified using barcoded V1 and V3 primers (B-
192 27F + MID; A1-357R; [supplementary table 1](#)) in a single batch prior to semiconductor
193 sequencing on a single Ion Torrent 316v2 chip exactly as described (Hill *et al.* 2015) and
194 [supplementary methods](#). Amplification, library preparation and sequencing were conducted in
195 a single batch. Sequence data are available at EBI-SRA (SRP067436 : PRJNA306097).

196 Sequence processing and bioinformatics

197 Resulting sequences were quality filtered in Python using Mothur (Schloss *et al.* 2009) with
198 the USEARCH algorithm (Edgar 2010) before performing closed-reference OTU picking in
199 QIIME 1.9.0 (Caporaso *et al.* 2010) using the Greengenes 13_8 reference database (DeSantis
200 *et al.* 2006). OTUs were clustered at a threshold of 97% and sequence taxa assignments and
201 chimera checking were performed in QIIME using uclust (Edgar 2010) and RDP classifier
202 version 2.2 (Wang *et al.* 2007). Permutational Multivariate Analysis of Variance
203 (PERMANOVA), Canonical Analysis of Principal Components (CAP), distance-based linear
204 modelling (distLM), were performed with fourth-root transforms of Bray Curtis distances
205 based upon OTU relative abundance, while the Mantel-based test RELATE was performed
206 with 999 permutations using a resemblance matrix of the fourth-root transformed Bray-Curtis
207 distances and pairwise physical distances. Default options were selected for CAP, including
208 performance of leave-one-out analyses, an iterative cross-validation of model robustness.
209 DistLM was performed using normalised predictor variables selected in stepwise protocol and
210 their influence evaluated in sequential tests with adjusted r^2 values. PRIMER
211 6/PERMANOVA+ (PRIMER-E Ltd) was used for all multivariate analyses, and one way
212 ANOVA was calculated in Minitab 15. Data visualizations of OTU relative abundances using
213 Microsoft Excel or PRIMER6/PERMANOVA and Adobe Illustrator are based upon
214 unmodified data.

215 Network Analysis

216 A vector was created for each OTU to represent the OTU's abundance in each of the 37
217 samples as indicated by the formula:

$$x_i = [x_{i1}, x_{i2}, \dots, x_{i37}] (i = 1, \dots, 755)$$

218 To reduce sequencing effort bias, x_i values < 5 was set to zero (Zhang *et al.* 2013) and OTU
219 vectors which contain less than 8 non-zero elements (20%) were removed to reduce false high
220 correlations (Berry & Widder 2014). A second set of vectors was created based on
221 environmental variables measured for each of the 37 samples. Pairwise Spearman correlations
222 between all vectors were calculated and the associated p-value corrected for multiple
223 comparisons with a Benjamini-Hochburg adjustment.

224 A community network was created based on significant correlations ($\rho > |0.7|$ and adjusted
225 $p < 0.05$) using package [iGraph] in R (Csardi & Nepusz 2006), incorporating both OTU
226 abundances and measures of environmental variables. Community detection was based on
227 random walk algorithm ("walktrap") in [iGraph] (Pons & Latapy 2005). Network parameters
228 were compared with the Erdős-Renyi random model of a network of equal size. For both
229 observed and random model communities, network parameters were calculated using the
230 [iGraph] package in R (Csardi & Nepusz 2006).

231 To identify keystone taxa, the community network structure was used to identify OTUs which
232 function as "bottlenecks" within the community, suggesting that they are central to
233 community structuring and/or function. Bottlenecks are here defined as nodes with highest
234 betweenness centrality, a count of the number times the bottleneck appears on the shortest
235 paths between all other pairs of nodes (Peura *et al.* 2015) and therefore a measure of their
236 connectivity within the co-occurrence network..

237

238

For Review Only

239 RESULTS

240 Semi-conductor sequencing of 16S rRNA genes from 37 cryoconite samples distributed over
241 the Foxfonna ice cap (Figure 1) generated 4 609 547 total reads. Following processing, 755
242 bacterial OTUs were assigned by GreenGenes taxonomy to 13 phyla and 2 candidate phyla
243 using a 97% similarity cut-off. It should be noted that results of preliminary T-RFLP
244 community profiling of 16S rRNA genes cross-verified those of 16S sequencing in terms of
245 spatial and environmental parameter prediction trends (data not shown) therefore T-RFLP
246 results are not reported further.

247

248 Community composition and relative abundance of higher grade taxa

249 OTUs representing 87-91% of total relative abundance (RA) in the four sectors could be
250 assigned to GreenGenes taxonomy (Figure 2; Supplementary Table 2). Across the cryoconite
251 of Foxfonna ice cap the following phyla dominated the sequence dataset; *Proteobacteria*
252 (28.3% RA), followed by *Actinobacteria* (21.8% RA), *Cyanobacteria* (18.4% RA),
253 *Bacteroidetes* (7.0% RA), *Chloroflexi* (5.5% RA), *Gemmatimonadetes* (4.85% RA) and
254 *Acidobacteria* (1.77% RA). Within individual sectors (Figure 2) *Proteobacteria* was the
255 abundant phylum in sectors G1-G4 with RAs of 31.5%, 24.5%, 28.9%, 29.2% respectively.
256 *Actinobacteria* on the other hand were the second most abundant in G1 (23.9% RA), G2
257 (22.9% RA) and G4 (24.7% RA). The phylum *Cyanobacteria* was second-most represented in
258 the sequence data from sector G3 (21.7% RA) and third in sectors G1 (20.0 % RA), G2
259 (14.6% RA) and G4 (17.5% RA). Within the *Proteobacteria*, *Betaproteobacteria* dominated
260 over other classes (16.2% RA) followed by *Alphaproteobacteria* (6.8% RA). No significant

261 differences were observed in the diversity indices for species richness (ANOVA, $F=0.4$, $p =$
262 0.754) and evenness value (ANOVA, $F=0.27$, $p=0.845$) between sectors.

263 Evidence for a moderate pairwise distance-decay relationship in bacterial community
264 structure

265 Potential pairwise distance-decay relationships in Bray-Curtis similarity of fourth-root
266 transformed OTU relative abundance and geographic distance were tested for with 666
267 pairwise combinations of holes at distances between 77-1664 metres. The distance-decay plot
268 of the overall community (Supplementary Figure 1) shows a weak relationship between
269 geographical distance (m) and community dissimilarity which is confirmed by RELATE
270 analysis, revealing a moderate spatial influence upon overall community structure ($\rho=0.275$,
271 $p=0.001$). This is accounted for by significant Spearman correlations (Table 1) for the
272 *Acidobacteria* ($\rho=0.256$, $p=0.012$), *Chloroflexi* ($\rho=0.36$, $p=0.001$), *Gemmatimonadetes* ($\rho=$
273 0.275 , $p = 0.025$), *Proteobacteria* ($\rho=0.188$, $p=0.045$), and unassigned taxa ($\rho=0.397$,
274 $p=0.001$).

275

276 Environmental influences on bacterial community structure

277 Canonical analysis of principal coordinates (Figure 3b) clearly differentiates between sectors
278 of the ice cap, assigning 78.3% of samples to the correct sector upon leave-one out analysis.
279 Moreover, PERMANOVA returns a highly significant sector effect (pseudo- $F^2= 3.0622$,
280 $p=0.001$ with 999 permutations). Pairwise PERMANOVA (Supplementary Table 3) reveals
281 each combination of sectors differ significantly ($t=1.48-2.27$, $p=0.001-0.007$) suggesting a
282 clear effect of ice cap surface position on the bacterial community structure. When split by

283 phylum, OTU relative abundances differed significantly for most phyla (Pseudo- $F=2.43-5.74$;
284 $p=0.001-0.007$) between sectors with the exception of *Acidobacteria* and *Thermi*.

285 Therefore, to evaluate the relative importance of environmental factors in structuring the
286 bacterial community, distance-based linear modelling (distLM; **Figure 3a**) was performed,
287 resulting in a model which explained 29.2% of the total variation in the first two distance-
288 based redundancy analysis axes. Stepwise selection of predicting variables identified
289 significant contributions ($p<0.01$) by parameters related to geographic position (Northings,
290 Eastings, elevation, slope and aspect), melting season duration (summer positive degree days
291 and hours, positive hours, number of hours with incident radiation,) and biotic factors
292 (chlorophyll *a* concentration and apparent cryoconite area) in marginal tests (**Supplementary**
293 **Table 4**). Of these, sequential tests revealed positive degree days in summer as the most
294 influential (contribution to adjusted $r^2=0.12$, pseudo- $F=6.07$, $p=0.001$) followed by slope
295 (contribution to adjusted $r^2=0.08$, pseudo- $F=4.93$, $p=0.001$) Northings (contribution to
296 adjusted $r^2=0.001$, pseudo- $F=2.43$, $p=0.001$), Apparent Cryoconite Area (contribution to
297 adjusted $r^2=0.03$, pseudo- $F=2.06$, $p=0.01$), and Eastings (contribution to adjusted $r^2=0.04$,
298 pseudo- $F=2.99$, $p=0.002$). Wetness, FAA, incident radiation, positive degree hours and
299 elevation did not contribute significantly ($p>0.05$) to the final model (adjusted $r^2=0.33$;
300 $r^2=0.52$; **Supplementary Table 5**).

301 OTU occupancy analysis reveals the cryoconite bacterial community is dominated by a
302 generalist core

303 To explore the distribution and dominance of specific bacterial taxa in cryoconite across the
304 Foxfonna ice cap, the mean relative abundance of OTUs (clustered at 97%) across all samples
305 was compared with the number of samples containing each OTU (i.e. occupancy; (Barberan *et*

306 *al.* 2012)). A clear pattern emerges (Figure 4) in that the cryoconite bacterial community is
307 strongly dominated by a small number of taxa. Of the 755 OTUs present in the dataset, only
308 16 OTUs are present at a mean RA per sample >1 %. The cross-sample cumulative RA of
309 these 16 OTUs is strongly correlated with mean RA (Pearson $r=0.99$, $p<0.0001$) indicating
310 minimal variation in their RA in sites across the ice cap. Strikingly, all 16 OTUs present at a
311 mean RA per sample >1% are present in at least 36 of the 38 cryoconite samples analysed,
312 and indeed in all 37 samples for 13 of those OTUs. Consequently, these 16 OTUs are
313 collectively considered a group of core taxa which is both ubiquitous and abundant within the
314 cryoconite bacterial community. BLAST-based closest environmental relatives (CER) and
315 closest named relatives (CNR) of core taxa (Supplementary Table 6) reveals the core OTUs
316 closely match uncultured sequences (CER %id 97-99%) mainly from cryospheric (13 OTUs)
317 and soil (3 OTUs) habitats worldwide and more distantly related to cultivated taxa from soil
318 (14 OTUs, CNR % id 88-98) plus Antarctic cyanobacteria (2 OTUs).

319 A long tail distribution of less abundant, variable occupancy, non-core taxa is also present
320 (Figure 4). Across both core and tail populations, mean RA is positively correlated with
321 occupancy (Spearman $r=0.77$, $p<0.001$). The tail population of the cryoconite bacterial
322 community on Foxfonna comprises OTUs affiliated to at least 9 phyla, including the
323 proteobacterial classes *Alpha-*, *Beta-*, *Delta* and *Gamma- proteobacteria*. The core OTUs
324 include representatives of *Actinobacteria* (5 OTUs), *Cyanobacteria* (2 OTUs), *Proteobacteria*
325 (one *Alphaproteobacteria* OTU, three *Betaproteobacteria* OTUs and one
326 *Gammaproteobacteria* OTU) and single OTUs from each of *Bacteroidetes*, *Chloroflexi*,
327 *Gemmatimonadetes* and an unassigned OTU. Of these OTUs, an OTU, denovo40205,
328 assigned to the filamentous cyanobacterial genus *Leptolyngbya* is very prominent, being
329 present in all 37 sites and at a mean RA (12.5%) four times greater than the next most

330 dominant OTUs, an actinobacterial taxon affiliated to *Microbacteriaceae* and a
331 *Betaproteobacteria* OTU, both present at 4.4-4.5% mean RA. All remaining core OTUs are
332 present at 1.0-2.9% mean RA and include an OTU affiliated to the filamentous cyanobacterial
333 genus *Phormidium* (1.14% mean RA, at 36 sites).

334 Core OTUs are stronger influences on tail and total OTU relative abundances than
335 environmental conditions

336 The effect of core OTU composition and environmental parameters on tail and total OTU
337 relative abundances was examined (Figure 5, Figure 6). Both core and tail OTU populations
338 are significantly different in relative abundance across all quadrats of the Foxfonna ice cap
339 (PERMANOVA; Pseudo- $F=4.42$, $p=0.001$; Pseudo- $F=3.021$, $p=0.001$ respectively; CAP
340 shown in Figure 6 b-c). The Bray-Curtis distance matrices of core and tail OTU RA exhibit a
341 much stronger correlation (RELATE; $\rho=0.88$, $p=0.001$) than to geographic distance
342 (RELATE; $\rho=0.29$, $p=0.01$; $\rho=0.27$, $p=0.001$). Therefore the interactions between core and
343 tail OTU populations with environmental parameters were examined with a view to
344 understanding the relative importance of core taxa and environmental conditions in shaping
345 the cryoconite bacterial community.

346 When applying distLM with a matrix of core OTU RAs as predictors of tail OTU RA patterns
347 (Figure 6), all 16 core OTUs were very significant contributors ($p=0.001-0.007$) in marginal
348 tests (Supplementary Table 7), with 10 of 16 core OTUs highly significant in the derived
349 model according to sequential tests (Supplementary Table 8). For consistency, each core OTU
350 is referred to by the most detailed taxonomic assignment made and the reference number of
351 the OTU assigned during OTU selection. This model (adjusted $r^2=0.57$; $r^2=0.76$) is
352 influenced most by an OTU assigned to *Sphingobacteriaceae* (hereafter referred to as

353 *Sphingobacteriaceae*-61341; contribution to adjusted $r^2=0.15$, pseudo- $F=7.43$, $p=0.001$)
354 followed by *Microbacteriaceae*-32521 (contribution to adjusted $r^2=0.11$, pseudo- $F=6.18$,
355 $p=0.001$), *Intrasporangiaceae*-46072 (contribution to adjusted $r^2=0.10$, pseudo- $F=5.27$,
356 $p=0.001$) with *Chloroflexi*-37757, *Intrasporangiaceae*-27964, *Gemmatimonadales*-59904,
357 *Phormidium*-45763, *Leptolyngbya*-40205, *Xanthomonadaceae*-51358 and
358 *Betaproteobacteria*-10679 in decreasing order of influence, yet remaining statistically
359 significant (Supplementary Table 8, $p=0.001-0.025$).

360 Considering the apparent strength of core OTU influence in shaping the tail population, the
361 relative influence of the core and environmental parameters upon the total and tail OTU
362 populations was tested (Figure 5, Figure 6). All 16 OTUs, and parameters relating to
363 Cartesian position, chlorophyll content and apparent cryoconite area and melt season duration
364 were significant predictors of total community structure ($p<0.05$) in marginal tests
365 (Supplementary Table 9) while parameters relating to energy receipt and melt (e.g. incident
366 radiation or wetness) were not, with the exception of hours of incident radiation. Sequential
367 tests (Supplementary Table 10) revealed the derived model (adjusted $r^2=0.60$; $r^2=0.84$) was
368 heavily influenced by seven core OTUs (cumulative $r^2=0.59$), principally
369 *Sphingobacteriaceae*-61341 (contribution to adjusted $r^2=0.17$, pseudo- $F=8.55$, $p=0.001$) and
370 *Microbacteriaceae*-32521 (contribution to adjusted $r^2=0.13$, pseudo- $F=7.35$, $p=0.001$)
371 followed by OTUs assigned to *Intrasporangiaceae*, *Leptolyngbya*, *Chloroflexi* and
372 *Phormidium* in decreasing order of influence. Subsequently, the three least influential (but
373 still statistically significant) predictors in the sequential tests were environmental parameters
374 relating to geographic position and hours of incident radiation (their cumulative adjusted
375 $r^2=0.04$, pseudo- $F=1.52-1.97$, $p=0.003-0.02$). The strong trend for core OTU influence to
376 predominate over the environmental parameters measured in shaping the bacterial community

377 is clearly paralleled in distLM prediction of tail population OTUs (Sequential tests:
378 Supplementary Table 11, dbRDA plot: Figure 6, Marginal tests: Supplementary Table 12)
379 with *Sphingobacteriaceae*-61341 (contribution to adjusted $r^2=0.17$, pseudo- $F=8.35$, $p=0.001$)
380 and *Microbacteriaceae*-32521 (contribution to adjusted $r^2=0.12$, pseudo- $F=7.05$, $p=0.001$)
381 again the strongest predicting variables of tail OTU structure. A total of 8 core OTUs plus
382 three environmental parameters (Cartesian position, hours of incident radiation) are
383 significant predictors of tail OTU structures.

384

385

386 OTU co-occurrence network analysis reveals modular sub-networks

387 Analysis of significant pairwise correlations between OTUs and environmental parameters
388 resulted in a relatively small network with 145 nodes and 304 edges. The observed network
389 was highly modular (observed = 0.77, Erdős-Renyi model = 0.41), with a considerably longer
390 average path length than expected from a random model of the same size (observed = 4.93,
391 Erdős-Renyi model = 3.58).

392 Environmental variables did not appear connected to most OTUs in the network, except for in
393 the case of one small cluster of OTUs disconnected from the remaining network. This cluster
394 was negatively correlated with several environmental variables related to energy inputs
395 including positive degree day sum (PDD), hours with temperature above 0°C (PositiveHrs)
396 and the positive degree day hours (PDhrs) (Figure 7).

397 The network contained several tightly clustered groups, disconnected or weakly connected
398 with the remaining community (Figure 7). Though there is some clustering of phylogenetic

399 groups, most groups are made up of OTUs from diverse taxa. Only one group is clearly
400 determined by phylogeny consisting of a small cluster of OTUs in the phylum *Cyanobacteria*.

401 Bottleneck OTUs as identified by the highest betweenness centrality score were dominated by
402 OTUs of the phylum *Actinobacteria* (top ten bottleneck OTUs: [Table 2](#)). All bottleneck OTUs
403 were connected to the largest cluster within the network through positive correlations, with
404 the exception of *Leptolyngbya*-40205. This OTU links a tight cluster of *Cyanobacteria* OTUs
405 through a negative correlation to OTUs in the largest network cluster ([Figure 7](#)). Six of the ten
406 top-scoring bottleneck OTUs are present within the core population (mean RA >1%).

407

408

409 DISCUSSION

410 The bacterial landscape of Foxfonna ice cap

411 Understanding the distributions of microbiota provides insights into the assembly,
412 biogeography and function of microbial communities across multiple scales (Bell 2010; Bell *et*
413 *al.* 2005). In the context of cryoconite ecosystems, understanding the spatial organization of
414 community composition provides insights into the microbial colonization of an extreme
415 environment, and the consequential interactions with melt responses of glacial ice surfaces.

416 Here we present the first bacterial biogeography of an ice cap. Semiconductor sequencing of
417 bacterial 16S rRNA genes amplified from cryoconite ecosystems distributed across an Arctic
418 ice cap reveals a cryoconite bacterial community dominated by a generalist core of (nearly-)
419 ubiquitous OTUs which influence the total and tail (i.e. non-core) bacterial community
420 structure. Chief among the core OTUs is a taxon assigned to the filamentous cyanobacterial
421 genus *Leptolyngbya* by the GreenGenes taxonomy. Co-occurrence network analyses reveal a
422 highly modular network which is constrained by bottleneck OTUs (Peura *et al.* 2015)
423 exhibiting high betweenness centrality scores. The ten top scoring OTUs are also members of
424 the core population. It is notable that the clearest phylogenetic signal within the network's
425 modules is apparent in a module comprised solely of cyanobacterial OTUs

426 Linking diversity analyses with geographical and other environmental parameters extracted
427 from a digital elevation model of the ice cap permits the elucidation of the physical factors
428 governing the assembly and structure of cryoconite bacterial communities. Distance-based
429 Linear Modelling reveals geographic position on the ice cap and melt season duration to be
430 better predictors of bacterial community structure than parameters relating to energy receipt
431 or surface hydrology. However, the structure of the core OTU population is a much better

432 predictor of both total and tail community structure than the measured environmental
433 parameters alone. The stronger influence of specific taxa rather than physical conditions on
434 the Foxfonna cryoconite microbiota is reflected within network analyses. Only two modules
435 within the network are linked to the physical parameters, but by negative correlations. The
436 analyses presented are highly coherent with the notion that cryoconite bacterial communities
437 develop as a consequence of autogenic ecosystem engineering (Cook *et al.* 2015b; Edwards *et*
438 *al.* 2014b) in the form of granular aggregation (Hodson *et al.* 2010; Langford *et al.* 2010). The
439 ubiquity and dominant abundance of OTU *Leptolyngbya*-40205 within the 16S sequencing
440 data are particularly consistent with a role as an ecosystem engineer. (Musilova *et al.* 2015)

441 However, the prominence of heterotrophic bacteria within the core and bottleneck OTU
442 populations is intriguing. In particular six OTUs assigned to the *Actinobacteria* accounting for
443 six of the top scoring bottleneck OTUs and five of those are present within the core
444 population. Of these, five are members of *Intrasporangiaceae*. While *Actinobacteria* have
445 been detected in previous studies of cryoconite bacteria (Edwards *et al.* 2011; Edwards *et al.*
446 2014b) this is the first time their prominent role in structuring the cryoconite bacterial
447 community has been invoked. Previous work has identified the predominance of *Alpha*- and
448 *Beta*- *proteobacteria* within cryoconite microbiota (Edwards *et al.* 2014b; Stibal *et al.* 2015).
449 While these are well-represented within the core population of Foxfonna cryoconite, they are
450 conspicuously absent from the bottleneck OTUs. We therefore infer that while taxa from
451 *Cyanobacteria* engineer the ecosystem and *Proteobacteria* contribute to heterotrophic
452 processes, certain *Actinobacteria* play a contrasting role by mediating key processes or biotic
453 interactions which affect overall community structure. Since keystone taxa are defined as taxa
454 which show influence upon a community or ecosystem beyond that expected from their
455 abundance (Power & Mills 1995) we consider these *Actinobacteria* OTUs as keystone taxa

456 and that biotic factors may play a hitherto unrecognized role in the formation of cryoconite
457 bacterial communities. Consequently, evaluating the relative roles of dispersal, environmental
458 and biotic filters in shaping the cryoconite bacterial community is merited.

459 How does dispersal filtering shape this bacterial community?

460 Contemporary microbial ecology literature is replete with studies inspired by Baas-Becking's
461 infamous statement (Baas-Becking 1934; De Wit & Bouvier 2006). A broad consensus may
462 be that some taxa are indeed cosmopolitan, while others exhibit biogeographical trends (van
463 der Gast 2015). For glaciers, the predominance of cosmopolitan taxa has been noted (Darcy *et al.*
464 2011; Franzetti *et al.* 2013) and previous work indicated distance-decay effects had
465 negligible influence in shaping the cryoconite biota of neighbouring valley glaciers (Edwards
466 *et al.* 2011). Since the Foxfonna ice cap is dome-shaped and not constrained by its
467 surrounding topography to face a given aspect, unlike valley glaciers, we hypothesised that
468 potential distance-decay effects would be revealed in this setting. Overall, there are
469 statistically significant but moderate distance-decay effects which consistent for both core and
470 tail populations, and are pronounced and significant for *Chloroflexi*, *Acidobacteria* and
471 *Gemmatimonadetes* in clear contrast to other phyla. It may be that specific traits in the life
472 history of these taxa condition their dispersal e.g.(Chu *et al.* 2011; DeBruyn *et al.* 2011).

473 Meanwhile, it is noteworthy that all core OTUs have closest environmental relatives
474 exhibiting >97% identity along the V1-V3 region of the 16S rRNA gene present in samples
475 from a global range of habitats which, with one exception, are from the cryosphere
476 (Supplementary Table 6). Coupled with their ubiquity across the ice cap, most probably due
477 to redistribution across the ice surface, this suggests an important trait of these core taxa is
478 their broad distribution across the cryosphere, thus promoting their likelihood of colonization,

479 resulting in a locally abundant and ubiquitous core population derived from a global pool of
480 propagules.

481

482 How does environmental filtering influence this bacterial community?

483 The second clause of Baas-Becking's statement (Baas-Becking 1934) directs the reader's
484 attention to the notion that prevailing environmental conditions influence microbial
485 community composition. Countless studies certainly support the importance of abiotic factors
486 in shaping microbial communities influenced by deterministic processes (e.g. (Wood *et al.*
487 2008)). The influence of surface hydrology and distance from the ice margin have been
488 inferred for valley glacier and ice sheet microbiota respectively (Edwards *et al.* 2011; Stibal *et*
489 *al.* 2015). Here, distLM consistently invoked physical parameters relating to geographic
490 position and melting season duration (either as positive degree days, [Supplementary Table 5](#);
491 or hours of incident radiation, [Supplementary Table 11](#)) as the strongest significant predictors
492 of community structures.

493 A common feature of all models was that factors relating to surface hydrology, either as
494 wetness of the ice surface or the extent of the FAA, failed to predict community structure.
495 Within the context of the Foxfonna ice cap, which resides at higher elevation and latitude,
496 with low mass balance gradients that exhibit strong inter-annual variability, this is plausible.
497 These conditions mean that community development may be curtailed to relatively brief
498 seasons of predominantly bare ice with a limited evolution of surface hydrological networks
499 and porous weathering crust ice at the surface, in contrast to cryoconite situated on strongly
500 ablating ice with longer growing seasons (Cook *et al.* 2015c; Irvine-Fynn & Edwards 2013).
501 While temporal analyses of cryoconite microbiota at the margin of the Greenland ice sheet

502 imply overall stability in community structure within melting seasons (Musilova *et al.* 2015)
503 we infer that the overall duration of melting season is an influential environmental parameter.
504 Further studies should directly examine the temporal evolution of cryoconite community
505 structures, particularly in conditions beyond those typical of the southwestern margin of
506 Greenland's ice sheet, and in so doing challenge the potential over-simplification of current
507 global models of cryoconite carbon cycling, which assume uniform rates of productivity
508 across a melting season of fixed duration (for example, 70 days: Anesio, *et al.*, (2009)).

509 How does biotic filtering in the form of taxon interactions influence the bacterial community?

510 Recognition that biotic filtering (i.e. taxon-taxon interactions such as competition,
511 cooperation and indeed ecosystem engineering) is an influential driver in the assembly of
512 environmental microbial communities is much more recent e.g. Goberna *et al.*, (2014). In the
513 context of glacial ecosystems, discourse regarding biotic filtering has been limited to
514 identifying algal taxa as primary colonizers of glacial surfaces e.g. Lutz *et al.* (2015) or the
515 role of filamentous cyanobacteria as putative ecosystem engineers or keystone species
516 (Edwards *et al.* 2014b). Here, we deduce that taxon interactions drive the assembly of
517 cryoconite communities colonizing the Foxfonna ice cap. The composition of the core
518 bacterial taxa is a strong predictor of the total and tail bacterial populations, with the
519 distributions of specific taxa proving better predictors than any physical parameters.
520 Moreover, the highly modular co-occurrence network is structured by nodes acting as
521 bottleneck OTUs (Table 2).

522 Congruent with prior work (Hodson *et al.* 2010; Langford *et al.* 2010), we find filamentous
523 cyanobacteria, specifically the OTU *Leptolyngbya*-40205 are important in the cryoconite
524 bacterial community, but while we concur they represent autogenic ecosystem engineers

525 (Edwards *et al.* 2014b; Langford *et al.* 2010; West 1990) they are less prominent as keystone
526 taxa. In contrast, selected *Actinobacteria* OTUs are prominent, highly-centralized bottleneck
527 OTUs within the highly modular co-occurrence network observed (Figure 6). We infer these
528 represent keystone taxa in that their influence exceeds their relative abundance within the
529 community profiled. Their positive co-occurrence with other taxa mitigates against their role
530 in competitive exclusion. Since their closest named relatives (Supplementary Table 6)
531 comprise taxa associated with soil humus we speculate these taxa may play roles in the
532 humification of dark organic matter associated with cryoconite (Takeuchi *et al.* 2001).

533 Others have interpreted phylogenetic clustering as evidence for biotic filtering (Goberna *et al.*
534 2014). The co-occurrence network derived here is modular in its nature, with taxonomically
535 diverse modules, a characteristic in common with taxon co-occurrence networks established
536 for other polar habitats, and interpreted as a sign of metabolic plasticity (Vick-Majors *et al.*
537 2014). Thus, the predominance of phylogenetically diverse modules may permit the
538 functional stability of the community in the face of its fluctuating environment. Most of these
539 modules exhibit phylum-level diversity with the exception of an exclusively cyanobacterial
540 module which is negatively correlated with the largest module, which houses all remaining
541 bottleneck OTUs. The disposition of the cyanobacterial module suggests that the autogenic
542 ecosystem engineers exert a limited influence upon community structure, unlike heterotrophic
543 bottleneck OTUs. Therefore, we contend that filamentous cyanobacteria, having engineered
544 the cryoconite ecosystem by the aggregation of aeolian organic matter and inorganic debris
545 (Hodson *et al.* 2010; Langford *et al.* 2010) are disconnected from the heterotrophic bacterial
546 community, which comprises closely interacting taxa. As such, the assembly of the cryoconite
547 bacterial community is biotically filtered with a primary succession from phototrophic taxa

548 associated with granule formation towards a highly interactive consortium of heterotrophic
549 bacteria which may act to humify the accumulated organic matter.

550 Technical considerations and limitations of the present study

551 This study focuses upon the intensive coverage of one ice cap in the High Arctic at a single
552 time-point and targets the bacterial community only. We note the presence of eukaryote and
553 viral communities in cryoconite(Sävström *et al.* 2002), beyond the scope of this study, as
554 well as reliable reports of Archaea associated with cryoconite, albeit from alpine and
555 Antarctic cryoconite(Cameron *et al.* 2012; Hamilton *et al.* 2013). The amplicon sequencing
556 dataset generated within this study did not reveal the presence of Archaea, and PCR assays
557 targeting Archaea did not generate specific amplicons (data not shown.) In line with other
558 work suggesting that Archaea are not detected in Arctic cryoconite (Cameron *et al.* 2012;
559 Edwards *et al.* 2011) we focused upon the bacterial community. Furthermore, analyses of
560 multiple time points and localities are likely to yield further insights to the structure and
561 function of glacial ecosystems (Edwards & Cook 2015). However, recent studies implying the
562 temporal stability of bacterial communities in cryoconite ecosystems (Musilova *et al.* 2015),
563 coupled with the cosmopolitan distribution of core taxa (Supplementary Table 6) documented
564 in a variety of cryospheric habitats imply the broader utility of insights from the Foxfonna ice
565 cap. The importance of melt season duration as a physical parameter predicting the bacterial
566 community structure is noted, and thus examination of cryoconite ecosystems in discrete
567 stages of melt season conditions is recommended, since this study sampled during the late
568 melt season.

569 Bulk DNA extraction coupled with amplicon semiconductor sequencing of the 16S rRNA
570 gene has been employed, in line with many other contemporary studies in microbial ecology

571 (Prosser 2012). Necessarily these studies all entail systematic biases in extraction,
572 amplification and sequencing (Lee *et al.* 2012). An important caveat here is that bulk DNA
573 extracts will include templates from active and inactive taxa (Blazewicz *et al.* 2013; Klein
574 2015) and thus the detection of temporal variation in activity levels is precluded (Stibal *et al.*
575 2015). Finally, processed reads were aligned to the GreenGenes taxonomy as described. It
576 should be noted that the highly dominant OTU, *Leptolyngbya*-40205, assigned to the genus
577 *Leptolyngbya* within the GreenGenes taxonomy possesses a closest named relative within an
578 Antarctic strain *Phormidesmis priestleyi* (95% id AY493581) which is also the closest relative
579 of Sanger-sequenced clone library Oscillatorean cyanobacterial OTUs from cryoconite
580 elsewhere on Svalbard (Edwards *et al.* 2011) and dominates the active bacterial community of
581 cryoconite on the south-western margin of the Greenland Ice Sheet (Cook *et al.* 2016). As the
582 phylogenetic placement of cyanobacteria from the cold biosphere improves (Christmas *et al.*
583 2015), so will the taxonomic affiliation of this cryoconite ecosystem engineer, which
584 currently resides within the *Phormidesmis*-like clade of cold adapted cyanobacteria.

585

586 Summary

587 We conclude that the assembly of the bacterial community of microbial-mineral aggregates
588 colonizing the High Arctic ice cap of Foxfonna is driven principally by biotic filtering. A
589 dominant generalist core of taxa emerges which includes filamentous cyanobacterial
590 ecosystem engineers and a discrete group of keystone taxa principally within the
591 *Actinobacteria*, likely humifying accumulated organic matter to darken the cryoconite. While
592 there is evidence for a moderate distance-decay effect in community similarity, it is notable
593 that the core taxa possess close environmental relatives from the global cryosphere, linking

594 microbial colonization processes interacting with glacier change at local scales with dispersal
595 within the cosmopolitan cold biosphere (Jungblut *et al.* 2009).

596

597 ACKNOWLEDGEMENTS

598 We gratefully acknowledge NERC NE/K000942/1 and AU University Research Fund to AE;
599 Great Britain Sasakawa Foundation to AE, NT, TI-F; NERC NE/G006253/1 to AJH; Welsh
600 Livery Guild scholarship to JSB; South African National Research Foundation Fellowship to
601 JKG. All authors thank the staff and students at UNIS for assistance with sample collection.

602 DATA ACCESSIBILITY

603 Sequence data are available at EBI-SRA (SRP067436 : PRJNA306097).

604 AUTHOR CONTRIBUTIONS

605 Conceived study: AJH, JKG, AE; conducted fieldwork: AE, TIF, JSB, NT, AJH; conducted
606 labwork: AE, JKG, PJW, APD; conducted data analyses: JKG ERS TIF LAJM AE; wrote
607 manuscript: JKG, ERS, TIF, AE. All authors contributed to and approved manuscript
608 submission.

609

610 TABLES AND FIGURES

611 TABLE 1: Spearman correlation between matrices of physical and Bray-Curtis distance by
612 phylum provided via RELATE analysis; significant correlations highlighted.

613 TABLE 2: Network bottlenecks identified as the OTUs with highest betweenness centrality
614 metrics. Node ID matches that used in figure 7.

615 FIGURE 1: Map of study location, the Foxfonna ice cap on Svalbard with (A) aerial overview
616 and (B) extracted digital elevation model, indicating sample points according to sector within
617 the figure key.

618 FIGURE 2: Phylum-level composition of 16S rRNA genes profiled by amplicon semi-
619 conductor sequencing and assigned to higher-grade taxa according to the GreenGenes
620 taxonomy (A) Sector G1; (B) Sector G2; (C) Sector G3; (D) Sector G4. The category
621 “Others” concatenates phyla present at a cumulative relative abundance <1% across the
622 dataset (Armatimonadetes, GN02, OD1, Thermi).

623 FIGURE 3: Ordination based analyses of Foxfonna ice cap bacterial communities (A)
624 distance-based redundancy analysis (dbRDA) ordination plot of distance-based linear models
625 of physical parameter predictors of bacterial community structure; (B) Canonical Analysis of
626 Principal Co-ordinates (CAP) of bacterial community structure according to a sector-based
627 model.

628 FIGURE 4: Occupancy plotting reveals that the Foxfonna ice cap cryoconite bacterial
629 communities (A) are dominated by a core of generalist taxa highlighted by box (exploded
630 view of core in inset B, annotated with OTU references). Bubble size is proportional to \log_{10}
631 of total RA and bubbles are shaded by taxonomic affiliation. Occupancy is defined by the
632 presence of an OTU within a site.

633 FIGURE 5: Distance-based redundancy analysis (dbRDA) ordination plot of distance-based
634 linear models (A) core OTU and environmental parameters on total community and (B) core
635 OTU and environmental parameters on tail community structure.

636 FIGURE 6: Distance-based redundancy analysis (dbRDA) ordination plot of distance-based
637 linear models (A) of core predictors of tail community structure and Canonical Analysis of

638 Principal Co-ordinates (CAP) of core and tail (panels B and C respectively) community
639 structures according to sector.

640

641 FIGURE 7: Community network based on significant pairwise Spearman correlations
642 between OTUs (green – positive correlation, orange – negative correlation). Size of node is
643 relative to average OTU abundance, while colour indicates OTU's phylum. Environmental
644 variables have been included as nodes in the network and are indicated as black squares.

645

646 **Table 1:** Spearman correlation between matrices of physical and Bray-Curtis distance by
 647 phylum provided via RELATE analysis; significant correlations highlighted.

Phylum	Rho	<i>p</i> value
<i>Acidobacteria</i>	0.256	0.012
<i>Actinobacteria</i>	0.123	0.114
<i>Armatimonadetes</i>	-0.019	0.549
<i>Bacteroidetes</i>	0.113	0.141
<i>Chloroflexi</i>	0.36	0.001
<i>Cyanobacteria</i>	0.154	0.065
<i>Gemmatimonadetes</i>	0.219	0.025
TM7	0.146	0.063
<i>Proteobacteria</i>	0.188	0.045
<i>Thermi</i>	0.094	0.174
Unassigned	0.397	0.001
WPS-2	0.079	0.233
OD1	0.086	0.203
GN02	-0.111	0.887

648

649

650 **Table 2** Network bottlenecks identified as the OTUs with highest betweenness centrality
 651 metrics. Node ID matches that used in figure 7.

Node ID	OTU	Phylum	Class	Order	Family	Genus	Centrality Mean	RA>1
D220	Denovo61555	<i>Actinobacteria</i>	<i>Acidimicrobiia</i>	<i>Acidimicrobiales</i>	C111		1318	
D106	Denovo37757	Chloroflexi	C0119				1261	+
D187	Denovo53638	<i>Actinobacteria</i>	<i>Actinobacteria</i>	<i>Actinomycetales</i>	<i>Intrasporangiaceae</i>		1102	+
D17	Denovo1447	<i>Actinobacteria</i>	<i>Actinobacteria</i>	<i>Actinomycetales</i>	<i>Intrasporangiaceae</i>		973	+
D175	Denovo51679	<i>Gemmatimonadetes</i>	<i>Gemmatimonadetes</i>	<i>Gemmatimonadales</i>	Ellin5301		915	
D160	Denovo48894	<i>Actinobacteria</i>	<i>Acidimicrobiia</i>	<i>Acidimicrobiales</i>	EB1017		660	+
D121	Denovo40205	<i>Cyanobacteria</i>	<i>Synechococcophycideae</i>	<i>Pseudanabaenales</i>	<i>Pseudanabaenaceae</i>	<i>Leptolyngbya</i>	619	+
D73	Denovo27964	<i>Actinobacteria</i>	<i>Actinobacteria</i>	<i>Actinomycetales</i>	<i>Intrasporangiaceae</i>		617	+
D185	Denovo53430						552	
D125	Denovo41255	<i>Actinobacteria</i>	<i>Actinobacteria</i>	<i>Actinomycetales</i>	<i>Intrasporangiaceae</i>		536	

652

653 **REFERENCES**

- 654 Anesio AM, Hodson AJ, Fritz A, Psenner R, Sattler B (2009) High microbial activity on
655 glaciers: importance to the global carbon cycle. *Global Change Biology* **15**, 955-960.
- 656 Baas-Becking LGM (1934) *Geobiologie; of inleiding tot de milieukunde* WP Van Stockum &
657 Zoon NV.
- 658 Barberan A, Bates ST, Casamayor EO, Fierer N (2012) Using network analysis to explore co-
659 occurrence patterns in soil microbial communities. *ISME j* **6**, 343-351.
- 660 Bell T (2010) Experimental tests of the bacterial distance-decay relationship. *ISME Journal* **4**,
661 1357-1365.
- 662 Bell T, Ager D, Song JI, *et al.* (2005) Larger islands house more bacterial taxa. *Science* **308**,
663 1884-1884.
- 664 Benn D, Evans DJ (2014) *Glaciers and glaciation* Routledge.
- 665 Berry D, Widder S (2014) Deciphering microbial interactions and detecting keystone species
666 with co-occurrence networks. *Frontiers in Microbiology* **5**:219
- 667 Blazewicz SJ, Barnard RL, Daly RA, Firestone MK (2013) Evaluating rRNA as an indicator
668 of microbial activity in environmental communities: limitations and uses. *The ISME*
669 *Journal* **7**, 2061-2068.
- 670 Bøggild C (1997) Different melt regimes indicated by surface albedo measurements at the
671 Greenland ice sheet margin—application of TM image. *EARSeL. Advances in remote*
672 *sensing* **5**, 82-88.
- 673 Cameron KA, Hodson AJ, Osborn AM (2012) Structure and diversity of bacterial, eukaryotic
674 and archaeal communities in glacial cryoconite holes from the Arctic and the
675 Antarctic. *FEMS microbiology ecology* **82**, 254-267.
- 676 Caporaso JG, Kuczynski J, Stombaugh J, *et al.* (2010) QIIME allows analysis of high-
677 throughput community sequencing data. *Nature Methods* **7**, 335-336.
- 678 Christmas NAM, Anesio A, Sanchez-Baracaldo P (2015) Multiple adaptations to polar and
679 alpine environments within cyanobacteria: a phylogenomic and Bayesian approach.
680 *Frontiers in Microbiology* **6**, 1070.
- 681 Chu H, Fierer N, Lauber CL, *et al.* (2011) Soil bacterial diversity in the Arctic is not
682 fundamentally different from that found in other biomes. *Environmental Microbiology*
683 **12**, 2998-3006.

- 684 Cook J, Edwards A, Bulling M, *et al.* (2016) Metabolome-mediated biocryomorphic
685 evolution promotes carbon fixation in Greenlandic cryoconite holes. *Environmental*
686 *Microbiology* Accepted article: DOI: 10.1111/1462-2920.13349.
- 687 Cook J, Edwards A, Hubbard A (2015a) Biocryomorphology: integrating microbial processes
688 with ice surface hydrology, topography and roughness. *Frontiers in Earth Science* **3**.
- 689 Cook JM, Edwards A, Takeuchi N, Irvine-Fynn TDL (2015b) Cryoconite: the dark biological
690 secret of the cryosphere. *Progress in Physical Geography* **46**, 66-111.
- 691 Cook JM, Hodson AJ, Irvine-Fynn TDL (2015c) Supraglacial weathering crust dynamics
692 inferred from cryoconite hole hydrology. *Hydrological Processes*, **30**, 433–446.
- 693 Csardi G, Nepusz T (2006) The igraph software package for complex network research.
694 *InterJournal, Complex Systems* **1695**, 1-9.
- 695 Darcy JL, Lynch RC, King AJ, Robeson MS, Schmidt SK (2011) Global Distribution of
696 *Polaromonas* Phylotypes - Evidence for a Highly Successful Dispersal Capacity. *Plos*
697 *One* **6**, e23742.
- 698 De Wit R, Bouvier T (2006) ‘Everything is everywhere, but, the environment selects’; what
699 did Baas Becking and Beijerinck really say? *Environmental Microbiology* **8**, 755-758.
- 700 DeBruyn JM, Nixon LT, Fawaz MN, Johnson AM, Radosevich M (2011) Global
701 biogeography and quantitative seasonal dynamics of *Gemmatimonadetes* in soil.
702 *Applied and Environmental Microbiology* **77**, 6295-6300.
- 703 DeSantis TZ, Hugenholtz P, Larsen N, *et al.* (2006) Greengenes, a chimera-checked 16S
704 rRNA gene database and workbench compatible with ARB. *Applied and*
705 *Environmental Microbiology* **72**, 5069-5072.
- 706 Edgar RC (2010) Search and clustering orders of magnitude faster than BLAST.
707 *Bioinformatics* **26**, 2460-2461.
- 708 Edwards A, Anesio AM, Rassner SM, *et al.* (2011) Possible interactions between bacterial
709 diversity, microbial activity and supraglacial hydrology of cryoconite holes in
710 Svalbard. *The ISME Journal* **5**, 150-160.
- 711 Edwards A, Cook S (2015) Microbial dynamics in glacier forefield soils show succession is
712 not just skin deep. *Molecular Ecology* **24**, 963-966.
- 713 Edwards A, Irvine-Fynn T, Mitchell AC, Rassner SME (2014a) A germ theory for glacial
714 systems? *Wiley Interdisciplinary Reviews: Water*. **1**, 331–340

- 715 Edwards A, Mur LAJ, Girdwood S, *et al.* (2014b) Coupled cryoconite ecosystem structure-
716 function relationships are revealed by comparing bacterial communities in Alpine and
717 Arctic glaciers *FEMS Microbiology Ecology* **89**, 222-237.
- 718 Edwards A, Pachebat JA, Swain M, *et al.* (2013a) A metagenomic snapshot of taxonomic and
719 functional diversity in an alpine glacier cryoconite ecosystem. *Environmental*
720 *Research Letters* **8**, 035003.
- 721 Edwards A, Rassner SM, Anesio AM, *et al.* (2013b) Contrasts between the cryoconite and
722 ice-marginal bacterial communities of Svalbard glaciers. *Polar Research* **32**, 19468.
- 723 Franzetti A, Tatangelo V, Gandolfi I, *et al.* (2013) Bacterial community structure on two
724 alpine debris-covered glaciers and biogeography of *Polaromonas* phylotypes. *The*
725 *ISME Journal* **7**, 1483–1492
- 726 Fuhrman JA (2009) Microbial community structure and its functional implications. *Nature*
727 **459**, 193-199.
- 728 Goberna M, García C, Verdú M (2014) A role for biotic filtering in driving phylogenetic
729 clustering in soil bacterial communities. *Global Ecology and Biogeography* **23**, 1346-
730 1355.
- 731 Griffiths RI, Whiteley AS, O'Donnell AG, Bailey MJ (2000) Rapid Method for Coextraction
732 of DNA and RNA from Natural Environments for Analysis of Ribosomal DNA- and
733 rRNA-Based Microbial Community Composition. *Applied and Environmental*
734 *Microbiology* **66**, 5488-5491.
- 735 Hamilton TL, Peters JW, Skidmore ML, Boyd ES (2013) Molecular evidence for an active
736 endogenous microbiome beneath glacial ice. *The ISME Journal*, **7**, 1402-12.
- 737 Hill R, Saetnan ER, Scullion J, *et al.* (2015) Temporal and spatial influences incur
738 reconfiguration of Arctic heathland soil bacterial community structure. *Environmental*
739 *Microbiology* doi: 10.1111/1462-2920.13017.
- 740 Hock R (2005) Glacier melt: a review of processes and their modelling. *Progress in Physical*
741 *Geography* **29**, 362-391.
- 742 Hodson A, Anesio AM, Ng F, *et al.* (2007) A glacier respire: quantifying the distribution and
743 respiration CO₂ flux of cryoconite across an entire Arctic supraglacial ecosystem.
744 *Journal of Geophysical Research* **112**, 9pp.

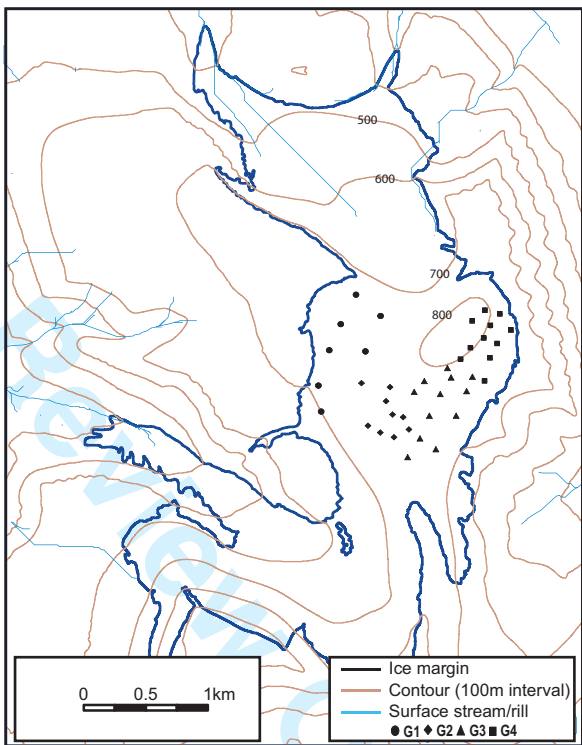
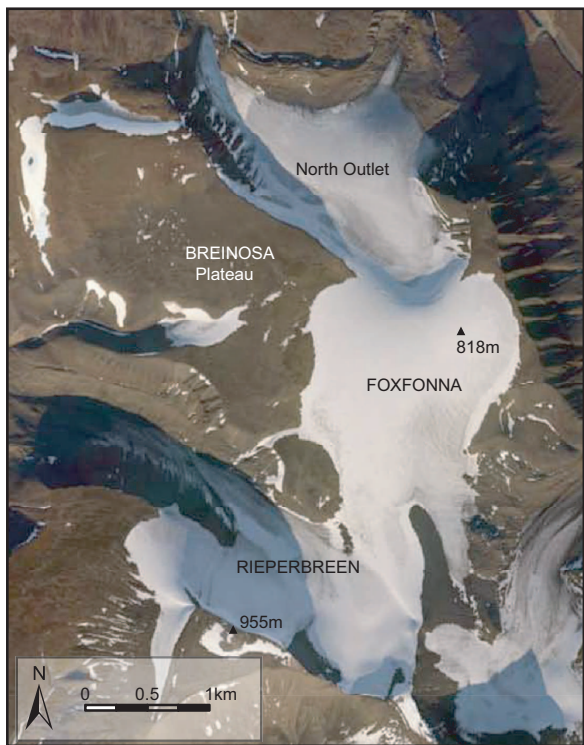
- 745 Hodson A, Anesio AM, Tranter M, *et al.* (2008) Glacial ecosystems. *Ecological Monographs*
746 **78**, 41-67.
- 747 Hodson A, Cameron K, Bøggild C, *et al.* (2010) The structure, biogeochemistry and
748 formation of cryoconite aggregates upon an Arctic valley glacier; Longyearbreen,
749 Svalbard. *Journal of Glaciology* **56**, 349-362.
- 750 Hood E, Battin TJ, Fellman J, O'Neel S, Spencer RGM (2015) Storage and release of organic
751 carbon from glaciers and ice sheets. *Nature Geoscience* **8**, 91-96.
- 752 Irvine-Fynn TDL, Bridge JW, Hodson AJ (2010) Rapid quantification of cryoconite: granule
753 geometry and in situ supraglacial extents, using examples from Svalbard and
754 Greenland. *Journal of Glaciology* **56**, 297-308.
- 755 Irvine-Fynn TDL, Edwards A (2013) A frozen asset: The potential of flow cytometry in
756 constraining the glacial biome. *Cytometry part A* **85**, 3-7.
- 757 Irvine-Fynn TDL, Hodson AJ, Moorman BJ, Vatne G, Hubbard AL (2011) Polythermal
758 glacier hydrology: A review. *Reviews in Geophysics*. **49**, RG4002.
- 759 Irvine-Fynn TD, Hanna E, Barrand N, *et al.* (2014) Examination of a physically based, high-
760 resolution, distributed Arctic temperature-index melt model, on Midtre Lovénbreen,
761 Svalbard. *Hydrological Processes* **28**, 134-149.
- 762 Jenson SK, Domingue JO (1988) Extracting topographic structure from digital elevation data
763 for geographic information system analysis. *Photogrammetric engineering and remote*
764 *sensing* **54**, 1593-1600.
- 765 Jungblut AD, Lovejoy C, Vincent WF (2009) Global distribution of cyanobacterial ecotypes
766 in the cold biosphere. *The ISME Journal* **4**, 191-202.
- 767 Klein DA (2015) Partial Formalization: An Approach for Critical Analysis of Definitions and
768 Methods Used in Bulk Extraction-Based Molecular Microbial Ecology. *Open Journal*
769 *of Ecology* **5**, 400.
- 770 Langford H, Hodson A, Banwart S, Bøggild C (2010) The microstructure and
771 biogeochemistry of Arctic cryoconite granules. *Annals of Glaciology* **51**, 87-94.
- 772 Langford HJ, Irvine-Fynn TDL, Edwards A, Banwart SA, Hodson AJ (2014) A spatial
773 investigation of the environmental controls over cryoconite aggregation on
774 Longyearbreen glacier, Svalbard. *Biogeosciences* **11**, 5365-5380.

- 775 Lee CK, Herbold CW, Polson SW, *et al.* (2012) Groundtruthing next-gen sequencing for
776 microbial ecology—biases and errors in community structure estimates from PCR
777 amplicon pyrosequencing.
- 778 Lutz S, Anesio AM, Edwards A, Benning LG (2015) Microbial diversity on Icelandic glaciers
779 and ice caps. *Frontiers in Microbiology* **6**, 307.
- 780 Moore ID, Grayson R, Ladson A (1991) Digital terrain modelling: a review of hydrological,
781 geomorphological, and biological applications. *Hydrological Processes* **5**, 3-30.
- 782 Musilova M, Tranter M, Bennett SA, Wadham JL, Anesio A (2015) Stable microbial
783 community composition on the Greenland Ice Sheet. *Frontiers in Microbiology* **6**, 193
- 784 Pedrós-Alió C (2006) Marine microbial diversity: can it be determined? *Trends in*
785 *microbiology* **14**, 257-263.
- 786 Peura S, Bertilsson S, Jones RI, Eiler A (2015) Resistant Microbial Cooccurrence Patterns
787 Inferred by Network Topology. *Applied and Environmental Microbiology* **81**, 2090-
788 2097.
- 789 Pons P, Latapy M (2005) Computing communities in large networks using random walks. In:
790 *Computer and Information Sciences-ISCIS 2005*, pp. 284-293. Springer.
- 791 Power ME, Mills LS (1995) The keystone cops meet in Hilo. *Trends in Ecology & Evolution*
792 **10**, 182-184.
- 793 Prosser JI (2012) Ecosystem processes and interactions in a morass of diversity. *FEMS*
794 *Microbiology Ecology* **81**, 507-519.
- 795 Rime T, Hartmann M, Brunner I, *et al.* (2015) Vertical distribution of the soil microbiota
796 along a successional gradient in a glacier forefield. *Molecular Ecology* **24**, 1091-108.
- 797 Rutter N, Hodson A, Irvine-Fynn T, Solas MK (2011) Hydrology and hydrochemistry of a
798 deglaciating high-Arctic catchment, Svalbard. *Journal of Hydrology* **410**, 39-50.
- 799 Sävström C, Mumford P, Marshall W, Hodson A, Laybourn-Parry J (2002) The microbial
800 communities and primary productivity of cryoconite holes in an Arctic glacier
801 (Svalbard 79°N). *Polar Biology* **25**, 591-596.
- 802 Schloss PD, Westcott SL, Ryabin T, *et al.* (2009) Introducing mothur: open-source, platform-
803 independent, community-supported software for describing and comparing microbial
804 communities. *Applied and Environmental Microbiology* **75**, 7537-7541.

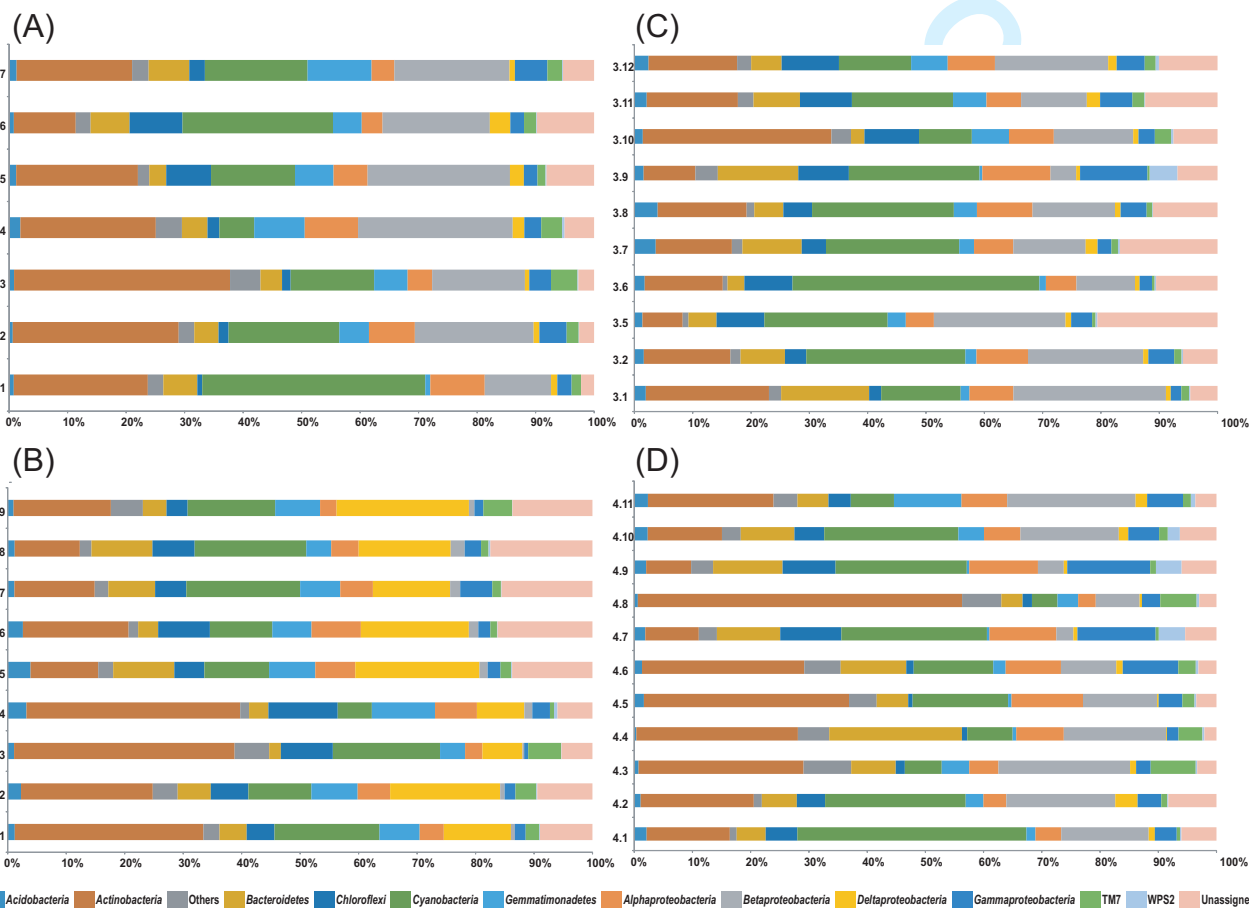
- 805 Segawa T, Ishii S, Ohte N, *et al.* (2014) The nitrogen cycle in cryoconites: naturally occurring
806 nitrification-denitrification granules on a glacier. *Environmental Microbiology* **16**,
807 3250-3262.
- 808 Steele JA, Countway PD, Xia L, *et al.* (2011) Marine bacterial, archaeal and protistan
809 association networks reveal ecological linkages. *The ISME Journal* **5**, 1414-1425.
- 810 Stibal M, Schostag M, Cameron KA, *et al.* (2015) Different bulk and active bacterial
811 communities in cryoconite from the margin and interior of the Greenland ice sheet.
812 *Environmental Microbiology Reports* **7**, 293-300.
- 813 Takeuchi N (2002) Optical characteristics of cryoconite (surface dust) on glaciers: the
814 relationship between light absorbency and the property of organic matter contained in
815 the cryoconite. *Annals of Glaciology* **34**, 409-414.
- 816 Takeuchi N, Kohshima S, Seko K (2001) Structure, formation, and darkening process of
817 albedo-reducing material (cryoconite) on a Himalayan glacier: a granular algal mat
818 growing on the glacier. *Arctic Antarctic and Alpine Research* **33**, 115-122.
- 819 Tarboton DG (1997) A new method for the determination of flow directions and upslope
820 areas in grid digital elevation models. *Water resources research* **33**, 309-319.
- 821 van der Gast CJ (2015) Microbial biogeography: the end of the ubiquitous dispersal
822 hypothesis? *Environmental Microbiology* **17**, 544-546.
- 823 Vick-Majors TJ, Priscu JC, Amaral-Zettler LA (2014) Modular community structure suggests
824 metabolic plasticity during the transition to polar night in ice-covered Antarctic lakes.
825 *The ISME Journal* **8**, 778-789.
- 826 Wadham J, Kohler J, Hubbard A, Nuttall AM, Rippin D (2006) Superimposed ice regime of a
827 high Arctic glacier inferred using ground-penetrating radar, flow modeling, and ice
828 cores. *Journal of Geophysical Research: Earth Surface (2003–2012)* **111**.
- 829 Wang Q, Garrity GM, Tiedje JM, Cole JR (2007) Naive Bayesian classifier for rapid
830 assignment of rRNA sequences into the new bacterial taxonomy. *Applied and*
831 *Environmental Microbiology* **73**, 5261-5267.
- 832 West NE (1990) *Structure and Function of Microphytic Soil Crusts in Wildland Ecosystems*
833 *of Arid to Semi-arid Regions* Academic Press.
- 834 Wise S (2000) Assessing the quality for hydrological applications of digital elevation models
835 derived from contours. *Hydrological Processes* **14**, 1909-1929.

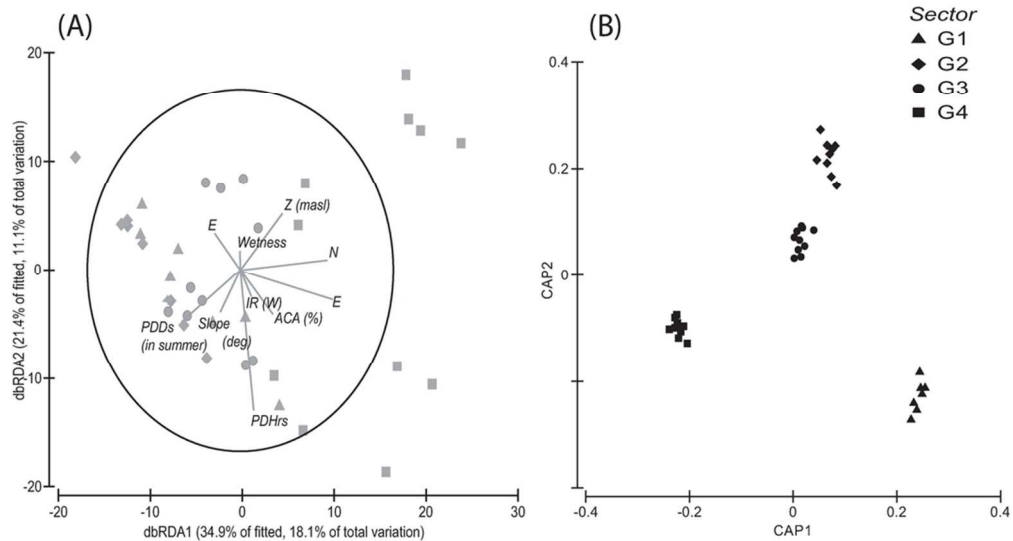
- 836 Wood SA, Rueckert A, Cowan DA, Cary SC (2008) Sources of edaphic cyanobacterial
837 diversity in the Dry Valleys of Eastern Antarctica. *The ISME Journal* **2**, 308-320.
- 838 Zhang S-W, Wei Z-G, Zhou C, Zhang Y-C, Zhang T-H (2013) Exploring the interaction
839 patterns in seasonal marine microbial communities with network analysis, 7th
840 International Conference on Systems Biology (ISB) 63-68. DOI:
841 10.1109/ISB.2013.6623795
- 842

For Review Only



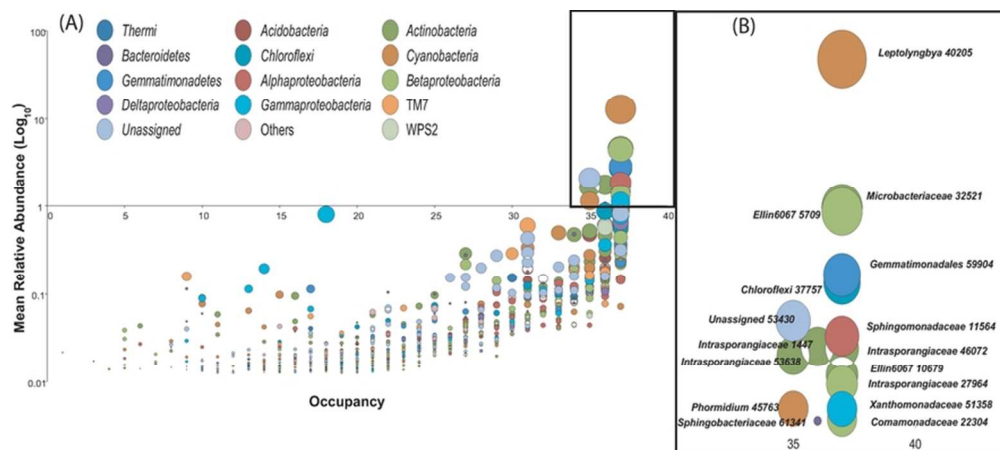
For Review





Ordination based analyses of Foxfonna ice cap bacterial communities (A) distance-based redundancy analysis (dbRDA) ordination plot of distance-based linear models of physical parameter predictors of bacterial community structure; (B) Canonical Analysis of Principal Co-ordinates (CAP) of bacterial community structure according to a sector-based model.

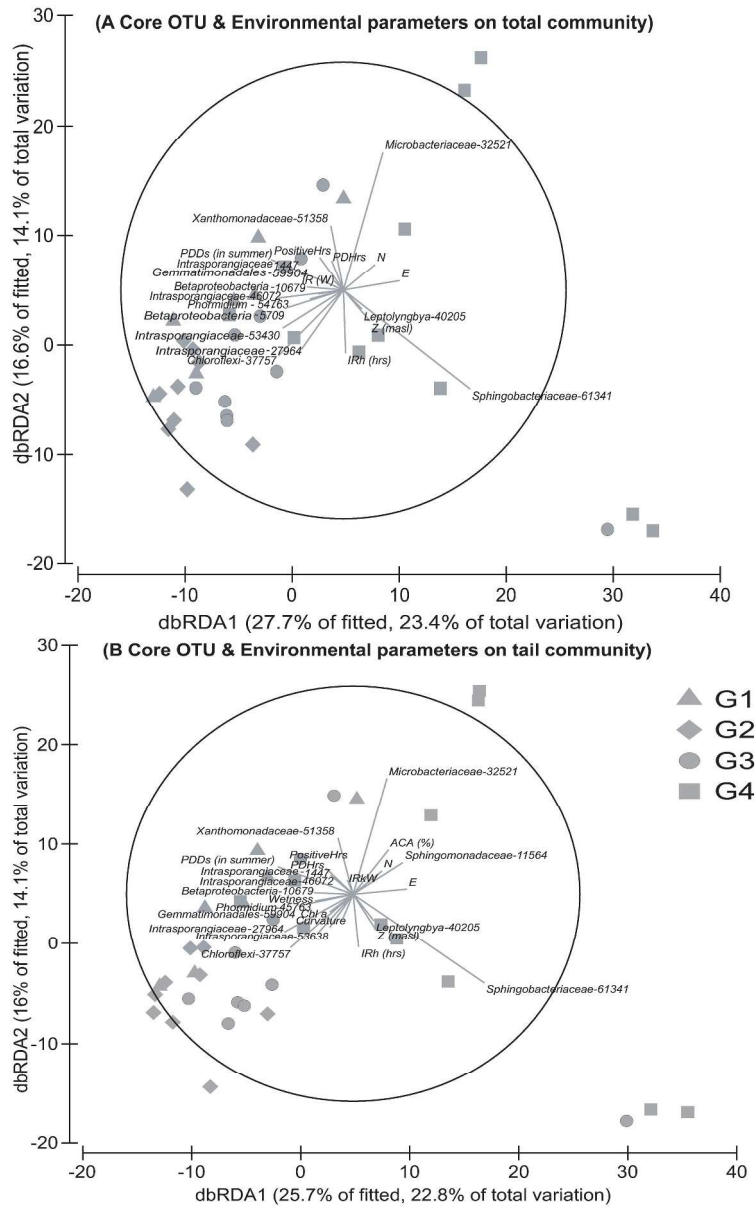
90x48mm (300 x 300 DPI)



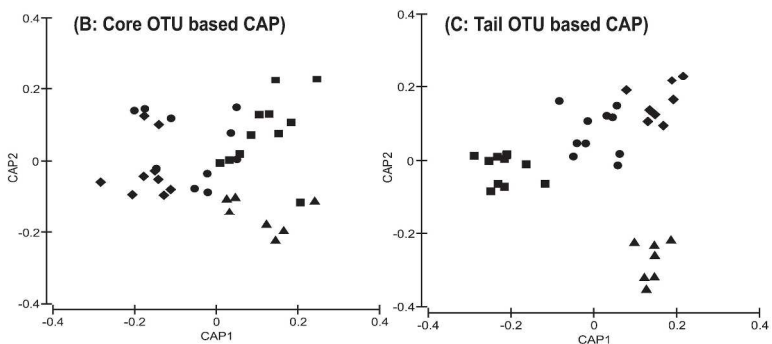
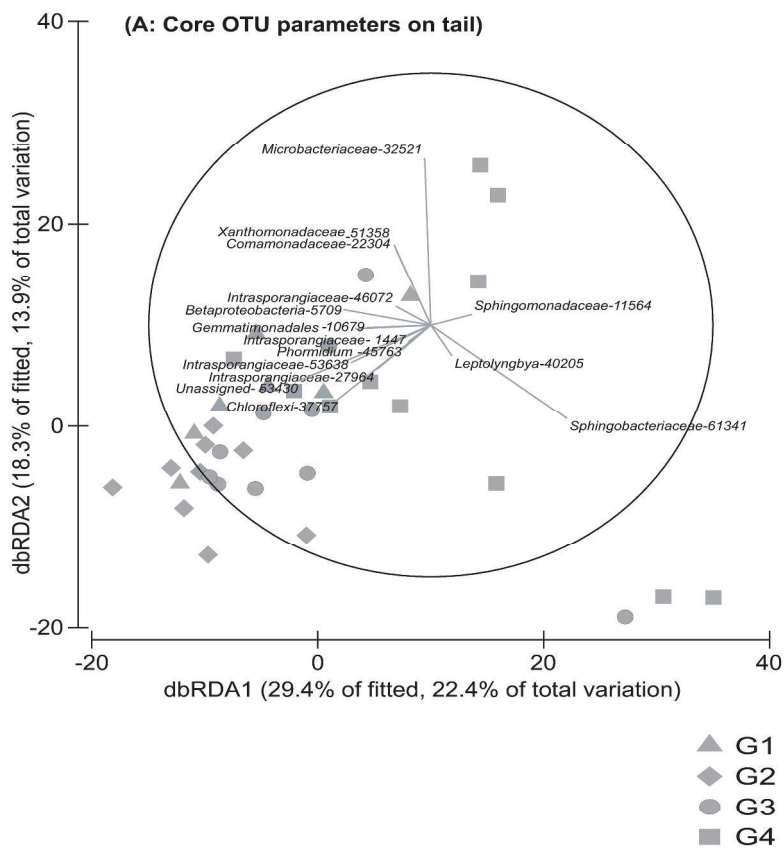
Occupancy plotting reveals that the Foxfonna ice cap cryoconite bacterial communities (A) are dominated by a core of generalist taxa highlighted by box (exploded view of core in inset B, annotated with OTU references). Bubble size is proportional to \log_{10} of total RA and bubbles are shaded by taxonomic affiliation. Occupancy is defined by the presence of an OTU within a site.

74x33mm (300 x 300 DPI)

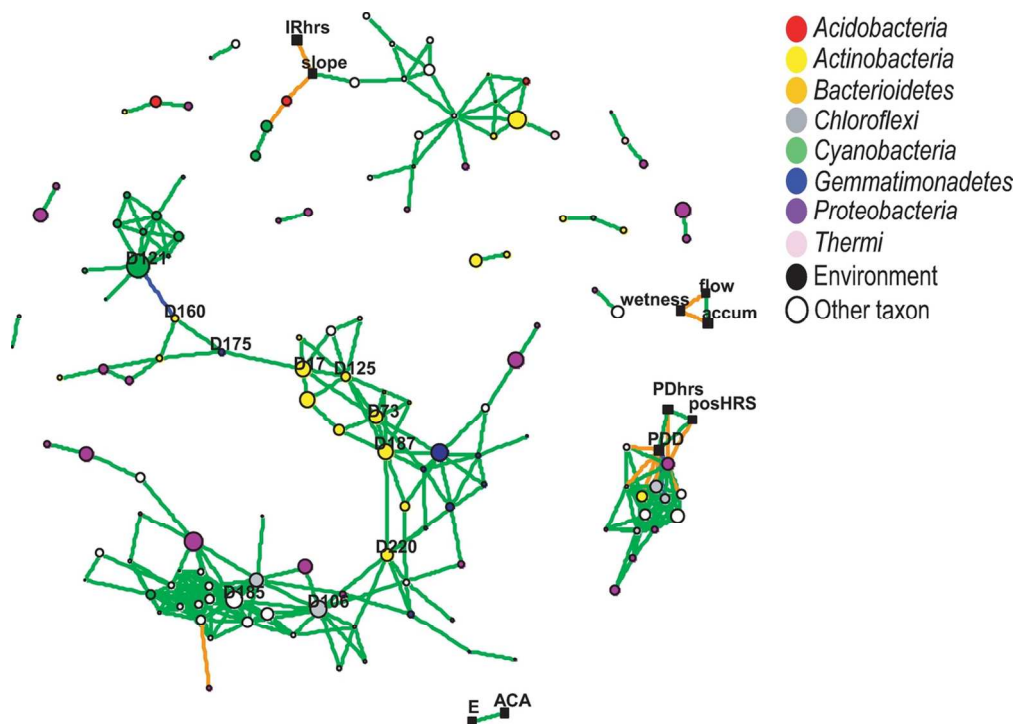
Review Only



Distance-based redundancy analysis (dbRDA) ordination plot of distance-based linear models (A) core OTU and environmental parameters on total community and (B) core OTU and environmental parameters on tail community structure. 246x396mm (300 x 300 DPI)



Distance-based redundancy analysis (dbRDA) ordination plot of distance-based linear models (A) of core predictors of tail community structure and Canonical Analysis of Principal Co-ordinates (CAP) of core and tail (panels B and C respectively) community structures according to sector.
244x379mm (300 x 300 DPI)



Community network based on significant pairwise Spearman correlations between OTUs (green – positive correlation, orange – negative correlation). Size of node is relative to average OTU abundance, while colour indicates OTU's phylum. Environmental variables have been included as nodes in the network and are indicated as black squares.
117x84mm (300 x 300 DPI)

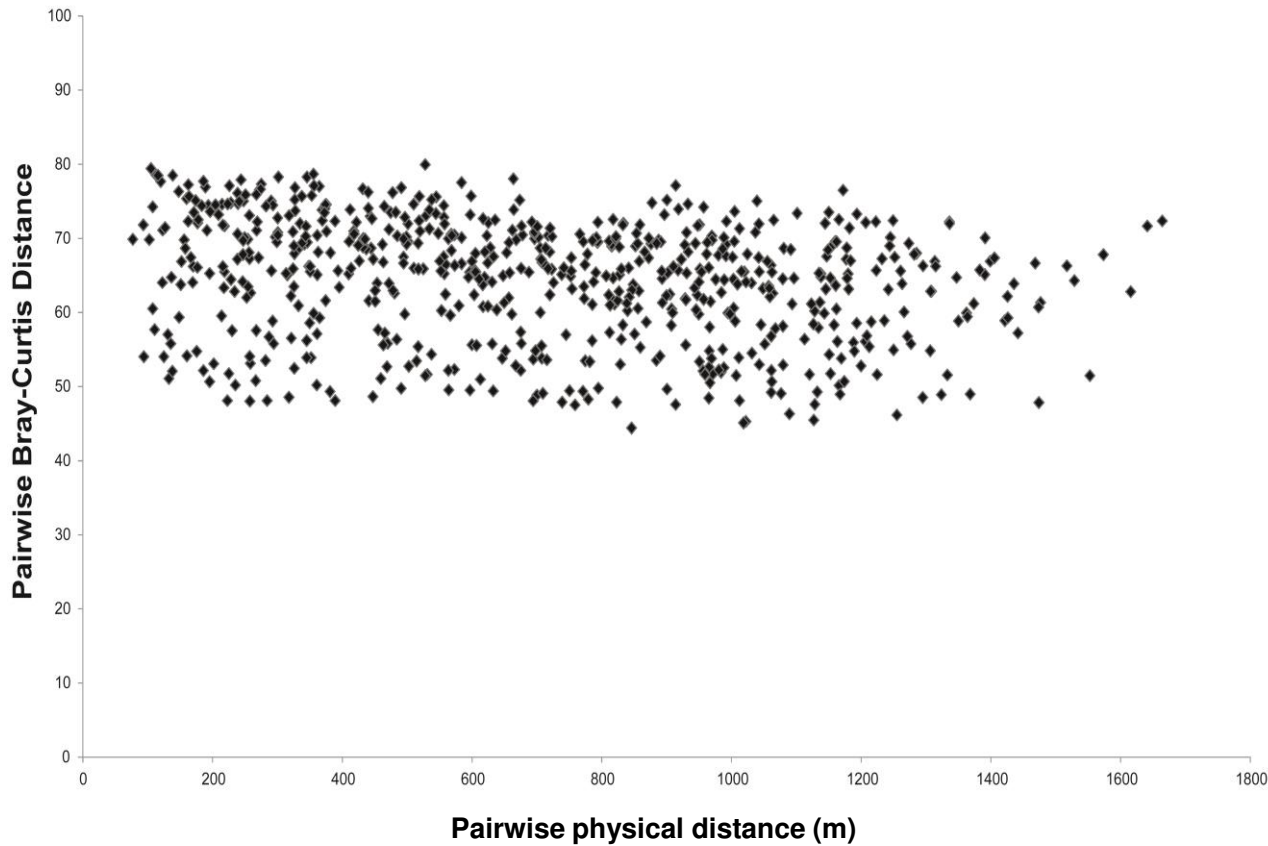
Only

Taxon interactions control the distributions of cryoconite bacteria colonizing a High Arctic ice cap

Jarishma K. Gokul, Andrew J. Hodson, Eli R. Saetnan, Tristram D.L., Irvine-Fynn, Philippa J. Westall, Andrew P. Detheridge, Nozomu Takeuchi, Jennifer Bussell Luis A.J. Mur, Arwyn Edwards.

SUPPLEMENTARY DATA:

Supplementary Figure 1: distance decay relationship between pairwise Bray Curtis distance between 16S sequencing profiles and pairwise physical distance.



Supplementary Table 1. Modified primers used for amplification of bacterial 16S rRNA gene regions (5'-3') V1-V3

Primer Name	Forward primer (Primer A-key) (30)	Ion Barcode (10)	Spacer	Template specific sequence-3' (19)	Notes
NGS_V1-V2_1	CCATCTCATCCCTGCGTGTCTCCGACTCAG	CTAAGGTAAC	GT	AGAGTTTGATCMTGGCTCAG	27F
NGS_V1-V2_2	CCATCTCATCCCTGCGTGTCTCCGACTCAG	TAAGGAGAAC	GT	AGAGTTTGATCMTGGCTCAG	
NGS_V1-V2_3	CCATCTCATCCCTGCGTGTCTCCGACTCAG	AAGAGGATTC	GT	AGAGTTTGATCMTGGCTCAG	
NGS_V1-V2_4	CCATCTCATCCCTGCGTGTCTCCGACTCAG	TACCAAGATC	GT	AGAGTTTGATCMTGGCTCAG	
NGS_V1-V2_5	CCATCTCATCCCTGCGTGTCTCCGACTCAG	CAGAAGGAAC	GT	AGAGTTTGATCMTGGCTCAG	
NGS_V1-V2_6	CCATCTCATCCCTGCGTGTCTCCGACTCAG	CTGCAAGTTC	GT	AGAGTTTGATCMTGGCTCAG	
NGS_V1-V2_7	CCATCTCATCCCTGCGTGTCTCCGACTCAG	TTCTGTATTC	GT	AGAGTTTGATCMTGGCTCAG	
NGS_V1-V2_8	CCATCTCATCCCTGCGTGTCTCCGACTCAG	TTCCGATAAC	GT	AGAGTTTGATCMTGGCTCAG	
NGS_V1-V2_9	CCATCTCATCCCTGCGTGTCTCCGACTCAG	TGAGCGGAAC	GT	AGAGTTTGATCMTGGCTCAG	
NGS_V1-V2_10	CCATCTCATCCCTGCGTGTCTCCGACTCAG	CTGACCGAAC	GT	AGAGTTTGATCMTGGCTCAG	
NGS_V1-V2_11	CCATCTCATCCCTGCGTGTCTCCGACTCAG	TCCTCGAATC	GT	AGAGTTTGATCMTGGCTCAG	
NGS_V1-V2_12	CCATCTCATCCCTGCGTGTCTCCGACTCAG	TAGTGGTTC	GT	AGAGTTTGATCMTGGCTCAG	
NGS_V1-V2_13	CCATCTCATCCCTGCGTGTCTCCGACTCAG	TCTAACGGAC	GT	AGAGTTTGATCMTGGCTCAG	
NGS_V1-V2_14	CCATCTCATCCCTGCGTGTCTCCGACTCAG	TTGGAGTGC	GT	AGAGTTTGATCMTGGCTCAG	
NGS_V1-V2_15	CCATCTCATCCCTGCGTGTCTCCGACTCAG	TCTAGAGGTC	GT	AGAGTTTGATCMTGGCTCAG	
NGS_V1-V2_16	CCATCTCATCCCTGCGTGTCTCCGACTCAG	TCTGGATGAC	GT	AGAGTTTGATCMTGGCTCAG	
NGS_V1-V2_17	CCATCTCATCCCTGCGTGTCTCCGACTCAG	TCTATTGTC	GT	AGAGTTTGATCMTGGCTCAG	
NGS_V1-V2_18	CCATCTCATCCCTGCGTGTCTCCGACTCAG	AGGCAATTGC	GT	AGAGTTTGATCMTGGCTCAG	
NGS_V1-V2_19	CCATCTCATCCCTGCGTGTCTCCGACTCAG	TTAGTCGGAC	GT	AGAGTTTGATCMTGGCTCAG	
NGS_V1-V2_20	CCATCTCATCCCTGCGTGTCTCCGACTCAG	CAGATCCATC	GT	AGAGTTTGATCMTGGCTCAG	
NGS_V1-V2_21	CCATCTCATCCCTGCGTGTCTCCGACTCAG	TCGCAATTAC	GT	AGAGTTTGATCMTGGCTCAG	
NGS_V1-V2_22	CCATCTCATCCCTGCGTGTCTCCGACTCAG	TTGAGAGCGC	GT	AGAGTTTGATCMTGGCTCAG	
NGS_V1-V2_23	CCATCTCATCCCTGCGTGTCTCCGACTCAG	TGCCACGAAC	GT	AGAGTTTGATCMTGGCTCAG	
NGS_V1-V2_24	CCATCTCATCCCTGCGTGTCTCCGACTCAG	AACCTCATTC	GT	AGAGTTTGATCMTGGCTCAG	
NGS_V1-V2_25	CCATCTCATCCCTGCGTGTCTCCGACTCAG	GATCTGCGAT	GT	AGAGTTTGATCMTGGCTCAG	
NGS_V1-V2_26	CCATCTCATCCCTGCGTGTCTCCGACTCAG	CAGCTCATCA	GT	AGAGTTTGATCMTGGCTCAG	
NGS_V1-V2_27	CCATCTCATCCCTGCGTGTCTCCGACTCAG	CAAACAACAG	GT	AGAGTTTGATCMTGGCTCAG	
NGS_V1-V2_28	CCATCTCATCCCTGCGTGTCTCCGACTCAG	GCAACACCAT	GT	AGAGTTTGATCMTGGCTCAG	
NGS_V1-V2_29	CCATCTCATCCCTGCGTGTCTCCGACTCAG	GCGATATATC	GT	AGAGTTTGATCMTGGCTCAG	
NGS_V1-V2_30	CCATCTCATCCCTGCGTGTCTCCGACTCAG	CGAGCAATCC	GT	AGAGTTTGATCMTGGCTCAG	
NGS_V1-V2_31	CCATCTCATCCCTGCGTGTCTCCGACTCAG	AGTCGTGCAC	GT	AGAGTTTGATCMTGGCTCAG	
NGS_V1-V2_32	CCATCTCATCCCTGCGTGTCTCCGACTCAG	GTATCTGCGC	GT	AGAGTTTGATCMTGGCTCAG	
NGS_V1-V2_33	CCATCTCATCCCTGCGTGTCTCCGACTCAG	CGAGGGCCCG	GT	AGAGTTTGATCMTGGCTCAG	
NGS_V1-V2_34	CCATCTCATCCCTGCGTGTCTCCGACTCAG	CAAATTCGGC	GT	AGAGTTTGATCMTGGCTCAG	
NGS_V1-V2_35	CCATCTCATCCCTGCGTGTCTCCGACTCAG	AGATTGACCA	GT	AGAGTTTGATCMTGGCTCAG	
NGS_V1-V2_36	CCATCTCATCCCTGCGTGTCTCCGACTCAG	AGTTACGAGC	GT	AGAGTTTGATCMTGGCTCAG	
NGS_V1-V2_37	CCATCTCATCCCTGCGTGTCTCCGACTCAG	GCATATGCAC	GT	AGAGTTTGATCMTGGCTCAG	
NGS_V1-V2_38	CCATCTCATCCCTGCGTGTCTCCGACTCAG	CAACTCCCGT	GT	AGAGTTTGATCMTGGCTCAG	
	Reverse primer (Primer P1-key) (23)				
PGM_V1-V2_Rev	CCTCTCATGGGACAGTCGGTGAT			CTGCTGCCTYCCGTA	357R

Supplementary Table 2: Diversity indices and environmental parameters measured

Sample	Number of OTUs	Pielou's evenness (J')	Shannon H'(loge)	Eastings (UTM)	Northings (UTM)	Chlorophyll a µg/g	Z (masl)	SLOPE (deg)	ASPECT (deg, 0=N clockwise)	FAA (m^2)	FLOWLENGTH (m)	CURVATURE	WETNESS	PDDs (in summer)	PositiveHrs	PDHrs	IR (W)	IRh (hrs)	IRkW	ACA (%)
1.1	476	0.64	3.97	526316	8672566	6.69	700.66	11.46	242.41	5075.00	1349.65	-8.69	0.002	77	1544	4379.4	525700	1659.4	525.7	3.41
1.2	512	0.74	4.61	526293	8672774	5.16	713.43	9.84	248.24	525.00	108.28	0.02	0.019	77	1507	4263.2	523400	1716.8	523.4	1.86
1.3	517	0.72	4.53	526380	8673063	4.04	738.02	7.64	265.13	4225.00	840.00	0.05	0.002	77	1438	4050.0	518100	1793.2	518.1	5.51
1.4	517	0.79	4.96	526472	8673272	5.96	746.95	5.91	292.91	75.00	12.07	-4.54	0.079	77	1416	3976.3	512000	1834.9	512	21.71
1.5	519	0.73	4.57	526630	8673519	9.09	736.29	7.40	6.65	2175.00	552.19	0.22	0.003	77	1443	4064.5	495000	1846.0	495	5.48
1.6	487	0.70	4.30	526789	8673341	5.90	761.18	7.60	344.10	175.00	32.07	-1.66	0.043	77	1380	3862.6	496300	1845.3	496.3	5.53
1.7	515	0.75	4.68	526670	8673046	5.97	769.58	4.80	270.38	2650.00	525.00	-4.88	0.002	77	1354	3797.4	520800	1821.7	520.8	5.01
2.1	474	0.70	4.33	526733	8672710	11.86	765.80	5.97	235.00	875.00	240.42	-3.31	0.007	77	1366	3826.6	529400	1756.2	529.4	10.63
2.2	526	0.76	4.77	526835	8672646	10.71	770.32	5.18	225.56	2425.00	678.82	0.02	0.002	77	1351	3791.8	530900	1771.8	530.9	5.00
2.3	412	0.65	3.91	526895	8672534	8.18	766.07	5.09	212.24	625.00	169.71	-1.54	0.008	77	1366	3824.5	532600	1761.9	532.6	9.53
2.4	492	0.74	4.61	526972	8672534	7.70	769.90	3.90	200.16	100.00	15.00	1.03	0.039	77	1352	3795.0	531600	1769.7	531.6	6.54
2.5	550	0.76	4.79	527013	8672440	5.83	763.33	5.37	190.19	850.00	165.00	0.07	0.006	77	1372	3845.7	535500	1751.2	535.5	9.02
2.6	508	0.73	4.55	526890	8672376	9.62	753.78	6.12	213.92	325.00	80.71	0.09	0.019	77	1392	3921.2	533500	1747.3	533.5	10.75
2.7	543	0.72	4.54	526777	8672378	10.56	745.87	7.01	225.11	900.00	245.42	0.01	0.008	77	1416	3985.1	532000	1734.6	532	9.69
2.8	519	0.73	4.58	526668	8672418	5.41	738.35	8.88	227.49	1400.00	388.91	0.04	0.006	77	1437	4047.3	533200	1696.3	533.2	7.15
2.9	487	0.70	4.31	526877	8672788	5.57	781.12	4.12	240.82	1400.00	378.55	-3.37	0.003	77	1311	3711.5	527400	1796.2	527.4	2.24
3.1	470	0.72	4.44	527537	8672831	7.82	775.99	8.45	142.28	725.00	197.99	0.30	0.012	77	1329	3749.2	539000	1691.4	539	4.95
3.2	508	0.70	4.36	527486	8672736	9.19	768.83	9.67	137.37	775.00	212.13	-3.00	0.012	77	1359	3803.2	538700	1659.6	538.7	4.42
3.5	498	0.67	4.16	527045	8672191	13.11	742.79	4.51	175.76	2475.00	490.00	0.12	0.002	77	1424	4010.5	532200	1767.2	532.2	5.36
3.6	472	0.59	3.65	527145	8672345	15.39	753.08	6.43	152.94	150.00	35.36	0.12	0.043	77	1394	3926.8	535700	1736.2	535.7	3.54
3.7	508	0.72	4.50	527187	8672514	6.20	767.40	6.89	152.90	75.00	14.14	0.04	0.092	77	1364	3814.2	537700	1719.3	537.7	5.76
3.8	508	0.71	4.39	527280	8672675	6.68	778.96	6.57	150.39	200.00	49.50	0.21	0.033	77	1315	3727.3	537300	1737.7	537.3	3.43
3.9	363	0.67	3.95	527335	8672826	5.55	790.62	4.96	153.38	1250.00	259.50	-1.72	0.004	76	1292	3643.4	534900	1751.2	534.9	3.42
3.1	525	0.75	4.69	527320	8672919	1.99	798.06	4.80	166.87	175.00	30.00	-3.86	0.027	76	1275	3591.1	536300	1763.3	536.3	4.05
3.11	524	0.77	4.80	527145	8672780	4.11	790.61	3.70	193.78	600.00	115.00	0.20	0.006	76	1292	3643.5	532900	1785.5	532.9	2.30
3.12	551	0.77	4.86	527077	8672700	4.93	784.68	3.57	187.34	525.00	100.00	0.25	0.007	76	1302	3685.8	532400	1787.1	532.4	2.43
4.1	503	0.64	3.99	527629	8672814	6.92	760.11	12.83	135.50	1200.00	332.34	-4.79	0.011	77	1384	3871.0	541000	1505.6	541	7.32
4.2	501	0.76	4.72	527674	8673000	3.53	778.42	11.06	128.27	1000.00	275.77	-2.05	0.011	77	1318	3731.2	537100	1646.3	537.1	2.68
4.3	447	0.76	4.65	527628	8673164	4.80	798.04	7.08	116.10	50.00	7.07	0.17	0.142	76	1275	3591.2	530300	1764.2	530.3	10.76
4.4	399	0.72	4.31	527729	8673119	5.90	782.33	10.84	117.11	525.00	141.42	-1.05	0.021	76	1308	3702.8	531400	1676.6	531.4	19.32
4.5	396	0.69	4.10	527845	8673224	5.20	769.05	11.63	107.42	1025.00	200.00	0.16	0.011	77	1356	3801.5	524900	1690.6	524.9	31.57
4.6	458	0.76	4.65	527755	8673356	1.98	789.52	8.95	104.60	700.00	135.00	-6.10	0.013	76	1293	3651.2	525200	1744.9	525.2	24.69
4.7	329	0.68	3.92	527634	8673387	3.05	802.25	3.63	58.27	200.00	49.50	-2.69	0.018	74	1263	3562.3	518800	1843.9	518.8	15.37
4.8	432	0.69	4.19	527533	8673301	3.04	805.80	0.47	67.50	375.00	70.00	-4.49	0.001	74	1259	3538.1	526300	1845.3	526.3	13.11
4.9	353	0.67	3.94	527439	8672989	9.89	799.16	5.03	147.00	225.00	56.57	0.23	0.022	74	1266	3583.5	534900	1773.9	534.9	6.90
4.1	515	0.78	4.85	527518	8673083	6.74	801.15	4.54	138.50	500.00	134.35	-1.00	0.009	74	1263	3569.8	532800	1776.9	532.8	5.32
4.11	489	0.78	4.81	527679	8673259	2.51	796.90	7.16	106.71	300.00	55.00	-1.02	0.024	76	1278	3599.2	526700	1768.8	526.7	2.92

Supplementary Table 3: Pairwise PERMANOVA comparison of bacterial community structure (at the OTU level) by sector of Foxfonna ice cap

Groups	t	P(perm)
G1, G4	1.6398	0.004
G1, G2	1.7124	0.001
G1, G3	1.5446	0.003
G4, G2	2.2761	0.001
G4, G3	1.5973	0.003
G2, G3	1.4803	0.007

Supplementary Table 4: Marginal tests from a distLM model of environmental predictors of bacterial community structure.

MARGINAL TESTS					
Variable	SS(trace)	Pseudo-F	P	Prop.	
E	2351.7	3.8009	0.001	9.80E-02	
N	2276.1	3.6659	0.001	9.48E-02	
Chl a ug/g	1380.4	2.1353	0.012	5.75E-02	
Z (masl)	1950.3	3.0947	0.002	8.12E-02	
SLOPE (deg)	2217.8	3.5625	0.002	9.24E-02	
ASPECT (deg, 0=N clockwise)	1861	2.9412	0.004	7.75E-02	
ACCUMAREA (m^2)	705.35	1.0595	0.355	2.94E-02	
FLOWLENGTH (m)	745.34	1.1214	0.283	3.10E-02	
CURVATURE	623.13	0.93268	0.474	2.60E-02	
WETNESS	538.76	0.80348	0.633	2.24E-02	
PDDs (in summer)	3549	6.0717	0.001	0.14783	
PositiveHrs	1915.8	3.0353	0.003	7.98E-02	
PDHrs	1826.8	2.8827	0.003	7.61E-02	
IR (W)	783.44	1.1807	0.238	3.26E-02	
IRh (hrs)	1579.3	2.4646	0.003	6.58E-02	
ACA (%)	1718.1	2.6979	0.012	7.16E-02	

Supplementary Table 5: Sequential tests from distLM model of environmental predictors of bacterial community structure. SS: sums of squares; Pseudo-F: test statistic

Variable	Adj R²	SS(trace)	Pseudo-F	P	Proportion explained	Cumulative variance
PDDs (in summer)	0.12	3549.0	6.1	0.001	0.15	0.15
SLOPE (deg)	0.21	2588.5	4.9	0.001	0.11	0.26
N	0.24	1248.6	2.5	0.001	0.05	0.31
ACA (%)	0.27	1005.9	2.1	0.011	0.04	0.35
E	0.31	1372.8	3.0	0.002	0.06	0.41
WETNESS	0.31	503.5	1.1	0.319	0.02	0.43
FAA (m²)	0.32	517.2	1.1	0.309	0.02	0.45
IRkW	0.32	459.1	1.0	0.399	0.02	0.47
PDHrs	0.33	661.2	1.5	0.106	0.03	0.50
Z (masl)	0.33	511.8	1.1	0.264	0.02	0.50
IR (W)	0.33	0.0	0.0	1.000	0.00	0.52

Supplementary Table 6: BLAST matches of core OTUs to closest environmental relatives (CER) and closest named relatives (CNR)

Core OTU	CER	CER #	CER %id	CER Habitat	CNR	CNR #	CNR %id	CER Habitat
Sphingobacteriaceae-61341	Uncultured actinobacterium clone IC4008	HQ622724.1	99	Svalbard ice	Pedobacter daechungensis	NR_041507	89	Korean lake sediment
Microbacteriaceae-32521	Frigoribacterium sp. MP117	KC256951	99	Tibetan glacier	Frigoribacterium sp. MP117	KC256951	99	Tibetan glacier
Intrasporangiaceae-46072	Uncultured bacterium clone ANTLV2_G12	DQ521529	98	Lake Vida ice, Antarctica	Oryzihumus sp. aerobe-19	KP185144	93	Korean grassland
Chloroflexi-37757	Uncultured bacterium clone gIs106	KC286738	98	Chinese glacier	Azospirillum sp. YM 195	GU396257.1	89	Sugarcane rhizome
Intrasporangiaceae-27964	Uncultured bacterium clone gs34	JF420640	97	German glacier sediment	Humibacter albus	AM494541	91	sewage sludge
Gemmatimonadales-59904	Uncultured bacterium clone NC54g8_19617	JQ377159	97	FACE soil	Ellin5220	AY234571	92	soil
Phormidium-45763	Uncultured cyanobacterium clone LJ14_522	KM112145	98	Antarctic microbial mat	Phormidium autumnale Ant-Ph68	DQ493874.1	98	Signy island, Antarctica
Leptolyngbya-40205	Uncultured bacterium clone IC4002	HQ622720	98	Svalbard ice	Phormidesmis priestleyi ANT.L66.	AY493581	95	Antarctica
Xanthomonadaceae-51358	Uncultured gamma proteobacterium clone TSC52	EU359963	98	Taiwanese soil	Pseudoxanthomonas sacheonensis	HF585486	94	US soil
Betaproteobacteria-10679	Uncultured bacterium isolate LH2-01	EU440469.1	98	Stromatolite, Canadian Arctic	Telluria mixta	LN794206	92	Germany
Intrasporangiaceae-53638	Uncultured bacterium clone LD_RB_26	EU644104	97	Siberian tundra	Ornithinimicrobium tianjinense	JQ948045	92	China
Betaproteobacteria-5709	Uncultured bacterium clone KuyT-ice-10	EU263777.1	97	Tibetan glacier	Massilia sp. 4106	JX566591.1	90	Chinese soil
Comamonadaceae-22304	Uncultured bacterium clone F35	FJ230911.1	98	Chinese river	Curvibacter	FN543107	98	Putative symbiont
Intrasporangiaceae-1447	Uncultured bacterium clone KuyT-IWPB-17	EU263719.1	99	Tibetan glacier	Eubacterium sp. 4c	AY216882	93	French peat
Sphingomonadaceae-11564	Uncultured bacterium clone GB7N87003GM6UD	HM728220	98	Antarctic soil	Novosphingobium sp. R1-11	KP182170	96	Korean soil
Unassigned-53430	Uncultured bacterium clone GB7N87003FR93L	HM732819.1	98	Antarctic soil	Rhizobium sp. AC86c1	AY776225.1	90	Ethiopian soil

Supplementary Table 7: Marginal tests from a distLM model of core predictors of tail population structure

MARGINAL TESTS					
Variable	SS(trace)	Pseudo-F	P	Prop.	
Leptolyngbya-40205	2026	2.9744	0.005	7.83E-02	
Microbacteriaceae-32521	3167.9	4.8847	0.001	0.12247	
Betaproteobacteria-5709	4014	6.4291	0.001	0.15518	
Gemmatimonadales-59904	3912.4	6.2373	0.001	0.15125	
Chloroflexi-37757	4394.3	7.1628	0.001	0.16988	
Unassigned-53430	4359.6	7.0947	0.001	0.16854	
Sphingomonadaceae-11564	2592.8	3.8991	0.001	0.10024	
Intrasporangiaceae-1447	2633.1	3.9666	0.002	0.1018	
Intrasporangiaceae-46072	2889.7	4.4018	0.001	0.11172	
Intrasporangiaceae-53638	3597.1	5.6533	0.001	0.13906	
Intrasporangiaceae-27964	3161.2	4.873	0.001	0.12221	
Betaproteobacteria-10679	2801	4.2502	0.001	0.10829	
Phormidium-45763	1723.9	2.4991	0.007	6.66E-02	
Xanthomonadaceae-51358	2411.6	3.5986	0.001	9.32E-02	
Comamonadaceae-22304	2725	4.1213	0.001	0.10535	
Sphingobacteriaceae-61341	4527.6	7.4262	0.001	0.17504	

Supplementary Table 8: Sequential tests from distLM model of core predictors of tail population structure

Variable	Adj R ²	SS(trace)	Pseudo- <i>F</i>	<i>P</i>	Proportion explained	Cumulative variance
<i>Sphingobacteriaceae-61341</i>	0.15147	4527.6	7.4262	0.001	0.175	0.17504
<i>Microbacteriaceae-32521</i>	0.26094	3284	6.1843	0.001	0.127	0.302
<i>Intrasporangiaceae-46072</i>	0.34344	2487.1	5.2721	0.001	0.096	0.39815
<i>Chloroflexi-37757</i>	0.40126	1801.3	4.187	0.001	0.070	0.46779
<i>Intrasporangiaceae-27964</i>	0.44508	1406.3	3.53	0.001	0.054	0.52215
<i>Gemmatimonadales-59904</i>	0.48589	1278.4	3.46	0.001	0.049	0.57158
<i>Phormidium-45763</i>	0.50599	788.11	2.22	0.001	0.030	0.60205
<i>Leptolyngbya-40205</i>	0.52088	654.59	1.90	0.002	0.025	0.62735
<i>Xanthomonadaceae-51358</i>	0.5314	548.33	1.63	0.005	0.021	0.64855
<i>Betaproteobacteria-10679</i>	0.53992	495.83	1.50	0.024	0.019	0.66772
<i>Intrasporangiaceae-53638</i>	0.54681	454.44	1.40	0.058	0.018	0.68529
<i>Betaproteobacteria-5709</i>	0.55312	434.32	1.35	0.074	0.017	0.70208
<i>Comamonadaceae-22304</i>	0.55863	412.16	1.30	0.112	0.016	0.71801
<i>Intrasporangiaceae-1447</i>	0.56352	394.48	1.26	0.139	0.015	0.73326
<i>Sphingomonadaceae-11564</i>	0.5677	376.68	1.21	0.187	0.015	0.74783
Unassigned-53430	0.5711	359.44	1.17	0.255	0.014	0.76172

Supplementary Table 9: Marginal tests from model M₁ model of environmental and core OTU predictors of total population structure

Variable	SS(trace)	Pseudo-F	P	Prop.
E	2351.7	3.8009	0.001	9.80E-02
N	2276.1	3.6659	0.001	9.48E-02
Chl a ug/g	1380.4	2.1353	0.019	5.75E-02
Z (masl)	1950.3	3.0947	0.003	8.12E-02
SLOPE (deg)	2217.8	3.5625	0.001	9.24E-02
ASPECT (deg, 0=N clockwise)	1861	2.9412	0.005	7.75E-02
ACCUMAREA (m^2)	705.35	1.0595	0.329	2.94E-02
FLOWLENGTH (m)	745.34	1.1214	0.271	3.10E-02
CURVATURE	623.13	0.93268	0.47	2.60E-02
WETNESS	538.76	0.80348	0.633	2.24E-02
PDDs (in summer)	3549	6.0717	0.001	0.14783
PostitiveHrs	1915.8	3.0353	0.003	7.98E-02
PDHrs	1826.8	2.8827	0.004	7.61E-02
IR (W)	783.44	1.1807	0.226	3.26E-02
IRh (hrs)	1579.3	2.4646	0.013	6.58E-02
IRkW	783.44	1.1807	0.258	3.26E-02
ACA (%)	1718.1	2.6979	0.01	7.16E-02
Leptolyngbya-40205	1725.2	2.7099	0.006	7.19E-02
Microbacteriaceae-32521	3062.2	5.1172	0.001	0.12756
Betaproteobacteria-5709	3148.9	5.2839	0.001	0.13117
Gemmatimonadales-59904	2730	4.4907	0.001	0.11372
Chloroflexi-37757	3180	5.344	0.001	0.13246
Unassigned-53430	2955.8	4.9144	0.001	0.12312
Sphingomonadaceae-11564	2736.5	4.5028	0.001	0.11399
Intrasporangiaceae-1447	1600.1	2.4993	0.014	6.67E-02
Intrasporangiaceae-46072	2090.7	3.3388	0.003	8.71E-02
Intrasporangiaceae-53638	2078.3	3.3172	0.005	8.66E-02
Intrasporangiaceae-27964	2223.5	3.5725	0.001	9.26E-02
Betaproteobacteria-10679	1582.9	2.4707	0.011	6.59E-02
Phormidium-45763	1317.8	2.0328	0.043	5.49E-02
Xanthomonadaceae-51358	1456.3	2.2602	0.009	6.07E-02
Comamonadaceae-22304	1625.1	2.5412	0.01	6.77E-02
Sphingobacteriaceae-61341	4713.8	8.5514	0.001	0.19635

Variable	Adj R ²	SS(trace)	Pseudo- <i>F</i>	<i>P</i>	Proportion explained	Cumulative variance
<i>Sphingobacteriaceae-61341</i>	0.173	4713.8	8.55	0.001	0.2	0.2
<i>Microbacteriaceae-32521</i>	0.3	3431.6	7.36	0.001	0.14	0.34
<i>Intrasporangiaceae-46072</i>	0.377	2158.9	5.2	0.001	0.09	0.43
<i>Intrasporangiaceae-27964</i>	0.419	1298	3.35	0.001	0.05	0.48
<i>Leptolyngbya-40205</i>	0.454	1108.7	3.04	0.001	0.05	0.53
<i>Chloroflexi-37757</i>	0.476	815.45	2.33	0.001	0.03	0.56
<i>Phormidium-45763</i>	0.496	726.07	2.16	0.001	0.03	0.59
N	0.512	643.2	1.98	0.003	0.03	0.62
E	0.526	570.53	1.8	0.002	0.02	0.64
IRh (hrs)	0.535	473.19	1.53	0.018	0.02	0.66
<i>Intrasporangiaceae -1447</i>	0.543	447.6	1.47	0.05	0.02	0.68
Unassigned-53430	0.549	403.23	1.34	0.085	0.02	0.7
<i>Betaproteobacteria-5709</i>	0.555	384.11	1.29	0.137	0.02	0.72
PDHrs	0.563	426.21	1.46	0.045	0.02	0.73
<i>Gemmatimonadales-59904</i>	0.57	379.04	1.32	0.133	0.02	0.75
IR (W)	0.574	349.92	1.23	0.19	0.01	0.76
<i>Xanthomonadaceae-51358</i>	0.579	347.69	1.24	0.188	0.01	0.78
<i>Betaproteobacteria-10679</i>	0.585	344.71	1.24	0.227	0.01	0.79
PositiveHrs	0.588	319.18	1.16	0.308	0.01	0.81
<i>Sphingomonadaceae-11564</i>	0.59	291.21	1.07	0.405	0.01	0.82
PDDs (in summer)	0.599	306.95	1.15	0.296	0.01	0.86
Z (masl)	0.602	290.48	1.09	0.352	0.01	0.87
<i>Sphingomonadaceae-11564</i>	0.602	264.4	1	0.459	0.01	0.86

Variable	Adj R ²	SS(trace)	Pseudo- <i>F</i>	<i>P</i>	Proportion explained	Cumulative variance
<i>Sphingobacteriaceae-61341</i>	0.17	4985.8	8.36	0.001	0.19	0.19
<i>Microbacteriaceae-32521</i>	0.292	3584.5	7.05	0.001	0.14	0.33
<i>Intrasporangiaceae-46072</i>	0.367	2287.7	5.03	0.001	0.09	0.42
<i>Intrasporangiaceae-27964</i>	0.408	1389.6	3.27	0.001	0.05	0.47
<i>Leptolyngbya-40205</i>	0.441	1172.5	2.92	0.001	0.05	0.52
<i>Chloroflexi-37757</i>	0.464	884.78	2.3	0.001	0.03	0.55
<i>Phormidium-45763</i>	0.483	791.69	2.13	0.001	0.03	0.58
N	0.5	700.72	1.95	0.002	0.03	0.61
E	0.513	623.48	1.78	0.005	0.02	0.63
<i>Intrasporangiaceae-1447</i>	0.523	526.4	1.53	0.022	0.02	0.66
IRh (hrs)	0.531	496.06	1.47	0.036	0.02	0.67
<i>Unassigned-53430</i>	0.537	441.15	1.33	0.09	0.02	0.69
PDHrs	0.542	414.92	1.26	0.168	0.02	0.71
<i>Betaproteobacteria-5709</i>	0.551	466.38	1.45	0.05	0.02	0.73
<i>Gemmatimonadales-59904</i>	0.556	408.67	1.28	0.165	0.02	0.74
IRkW	0.561	383.75	1.22	0.202	0.01	0.76
<i>Xanthomonadaceae-51358</i>	0.566	379.77	1.22	0.208	0.01	0.77
Z (masl)	0.571	379.05	1.23	0.208	0.01	0.79
<i>Betaproteobacteria-10679</i>	0.574	346.03	1.13	0.328	0.01	0.8
WETNESS	0.576	334.33	1.1	0.344	0.01	0.81
<i>Sphingomonadaceae-11564</i>	0.577	313.92	1.03	0.421	0.01	0.82
<i>Intrasporangiaceae-53638</i>	0.581	341.19	1.13	0.342	0.01	0.84
ACA (%)	0.582	312.92	1.04	0.443	0.01	0.85
PDDs (in summer)	0.587	344.06	1.16	0.324	0.01	0.86
CURVATURE	0.592	328.7	1.12	0.36	0.01	0.88
Chlorophyll a $\mu\text{g g}^{-1}$	0.592	296.43	1.01	0.45	0.01	0.89
PositiveHrs	0.593	298.39	1.02	0.438	0.01	0.9
<i>Betaproteobacteria-5709</i>	0.593	291.84	1	0.474	0.01	0.89

Supplementary Table 12: Marginal tests from a distLM model of environmental and core OTU predictors of tail population structure

Variable	SS(trace)	Pseudo-F	P	Prop.
E	2472.3	3.6988	0.001	0.10
N	2445.5	3.65E+00	0.001	0.09
Chl a ug/g	1499.8	2.15E+00	0.021	0.06
Z (masl)	2101.1	3.09E+00	0.002	0.08
SLOPE (deg)	2369	3.53E+00	0.001	0.09
ASPECT (deg, 0=N clockwise)	1969.2	2.88E+00	0.001	0.08
ACCUMAREA (m^2)	769.03	1.07E+00	0.318	0.03
FLOWLENGTH (m)	812.22	1.13E+00	0.289	0.03
CURVATURE	668.69	9.29E-01	0.477	0.03
WETNESS	599.19	8.30E-01	0.59	0.02
PDDs (in summer)	3771.8	5.97E+00	0.001	0.15
PostitiveHrs	2064.1	3.04E+00	0.002	0.08
PDHrs	1969.8	2.89E+00	0.003	0.08
IR (W)	825.09	1.15E+00	0.25	0.03
IRh (hrs)	1654.7	2.39E+00	0.008	0.06
IRkW	825.09	1.15E+00	0.275	0.03
Irhrs	1653.8	2.39E+00	0.013	0.06
ACA (%)	1802.4	2.62E+00	0.007	0.07
Leptolyngbya-40205	1809	2.6319	0.008	0.07
Microbacteriaceae-32521	3228	4.99E+00	0.001	0.12479
Betaproteobacteria-5709	3288	5.10E+00	0.001	0.12712
Gemmatimonadales-59904	2803.4	4.25E+00	0.001	0.10838
Chloroflexi-37757	3354	5.21E+00	0.001	0.12967
Unassigned-53430	3136.9	4.83E+00	0.001	0.12127
Sphingomonadaceae-11564	2850.5	4.33E+00	0.001	0.1102
Intrasporangiaceae-1447	1672.1	2.42E+00	0.019	6.46E-02
Intrasporangiaceae-46072	2197.4	3.25E+00	0.005	8.50E-02
Intrasporangiaceae-53638	2191.5	3.24E+00	0.006	8.47E-02
Intrasporangiaceae-27964	2328.9	3.46E+00	0.004	9.00E-02
Betaproteobacteria-10679	1639.1	2.368	0.016	6.34E-02
Phormidium-45763	1390.3	1.99E+00	0.042	5.38E-02
Xanthomonadaceae-51358	1559.1	2.2449	0.006	6.03E-02
Comamonadaceae-22304	1729.1	2.51E+00	0.007	6.68E-02
Sphingobacteriaceae-61341	4985.8	8.36E+00	0.001	0.19275